Facies (2016) 62:22
DOI 10.1007/s10347-016-0473-9

ORIGINAL ARTICLE

Rocking around a volcanic island shelf: Pliocene Rhodolith beds from Malbusca, Santa Maria Island (Azores, NE Atlantic)

Ana Cristina Rebelo[1,2,3,4] · Michael W. Rasser[4] · Andreas Kroh[5] · Markes E. Johnson[6] · Ricardo S. Ramalho[7] · Carlos Melo[3,8] · Alfred Uchman[9] · Björn Berning[10] · Luís Silva[1,2] · Vittorio Zanon[11,12] · Ana I. Neto[1,13] · Mário Cachão[14] · Sérgio P. Ávila[1,2,3]

Received: 25 November 2015 / Accepted: 1 June 2016 / Published online: 20 June 2016

Abstract Rhodoliths are a common producer of carbonates on modern and ancient shelves worldwide, and there is growing evidence that they thrive on volcanic insular shelves. However, little is still known on how rhodoliths cope with the demands of this particularly dynamic environment. In this study, the focus is placed on fossil rhodoliths from a Pliocene sequence at Santa Maria Island, Azores, in order to gain further insight into the life cycle (and death) of rhodoliths living within a mid-ocean active volcanic setting. These rhodoliths occur as a massive accumulation within a larger submarine volcano-sedimentary sequence that was studied from the macro- to the microscale in order to reconstruct the paleoenvironmental conditions under which the rhodolith accumulation was deposited and buried. All fossil rhodoliths from this setting are multi-specific and demonstrate robust growth forms with a lumpy morphology. Moreover, taphonomical analyses show the succession of several destructive events during rhodolith growth, suggesting life under a highly dynamic system prior to stabilization and burial. The rhodoliths therefore tell a story of an eventful life, with multiple transport and growth stages, owing to the environment in which they lived. Transport and deposition to their final resting place was storm-associated, as supported by the general sedimentary sequence. In particular, the sequence features an amalgamation of tempestites deposited under increasing water depths, sediment aggradation, and before burial by volcanic activity. This transgressive trend is also attested by the overall characteristics of the volcano-sedimentary

✉ Ana Cristina Rebelo
acfurtadorebelo@gmail.com

[1] Departamento de Biologia, Universidade dos Açores, Campus de Ponta Delgada, Apartado, 1422-801 Ponta Delgada, Açores, Portugal

[2] CIBIO–Centro de Investigação em Biodiversidade e Recursos Genéticos, InBIO Laboratório Associado, Pólo dos Açores–Departamento de Biologia da Universidade dos Açores, 9501-801 Ponta Delgada, Açores, Portugal

[3] MPB–Marine PalaeoBiogeography Working Group of the University of the Azores, Rua Mãe de Deus, Portugal

[4] SMNS–Staatliches Museum für Naturkunde Stuttgart, Rosenstein 1, 70191 Stuttgart, Germany

[5] Geologisch-Paläontologische Abteilung, Naturhistorisches Museum Wien, Burgring 7, 1010 Vienna, Austria

[6] Department of Geosciences, Williams College, Williamstown, MA 01267, USA

[7] School of Earth Sciences, University of Bristol, Wills Memorial Building, Queen's Road, Bristol BS8 1RJ, UK

[8] Departamento de Geociências, Universidade dos Açores, Campus de Ponta Delgada, Apartado, 1422-801 Ponta Delgada, Açores, Portugal

[9] Institute of Geological Sciences, Jagiellonian University, Oleandry 2a, 30-063 Kraków, Poland

[10] Oberösterreichisches Landesmuseum, Geowissenschaftliche Sammlungen, Welser Str. 20, 4060 Leonding, Austria

[11] Centro de Vulcanologia e Avaliação de Riscos Geológicos, Universidade dos Açores, 9501-801 Ponta Delgada, Açores, Portugal

[12] Institut de Physique du Globe de Paris, 1, Rue Jussieu, 75238 Paris Cedex 05, France

[13] Grupo de Investigação em Ecologia Aquática de Sistemas Insulares do Grupo de Biodiversidade dos Açores, cE3c - Centro de Ecologia, Evolução e Alterações Ambientais, Universidade dos Açores, Rua Mãe de Deus, 9501-801 Ponta Delgada, Portugal

[14] Instituto Dom Luiz, Faculdade de Ciências da Universidade de Lisboa, 1749-016 Lisbon, Portugal

succession, which exhibits the transition to subaerial environment in excess of 100 m above the rhodolith bed.

Keywords Coralline red algae · Peyssonneliacean algae · Early Pliocene · Paleoenvironment · Azores Archipelago

Introduction

Rhodoliths are carbonate nodules built by free-living coralline red algae (Rhodophyta) around a central core, often a pebble or shell fragment. These structures are unattached and roll around the sea floor under the influence of waves, currents and/or bioturbation, which promotes a more-or-less equitable exposure to sunlight, essential for photosynthesis. In general, rhodoliths are widespread among non-tropical and tropical marine environments where they can live in various water depths, from tidal pools down to greater water depths within the photic zone (Bourrouilh-Le Jan and Hottinger 1988; Checconi et al. 2010). Rhodoliths have been widely reported from continental shelves and continental island shelves (Bosence 1983; Checconi et al. 2010; Basso et al. 2009), but growing evidence shows that these organisms also thrive on oceanic island shelves, both volcanically inactive and active (Johnson et al. 2014 and references therein).

Reefless island shelves are particularly dynamic marine environments due to their exposure to strung surf, storms, volcanism, and mass wasting; additionally, reefless island shelves are also narrower and steeper than continental shelves, a condition that facilitates sediment transport and greatly contributes to environmental instability. How rhodoliths cope with environmental pressures of this dynamic environment is, however, relatively unknown, and therefore the focus of this study.

The Malbusca section on Santa Maria Island (Azores, NE Atlantic) essentially corresponds to a volcano-sedimentary sequence comprising submarine effusive products and beds of clastic sediments. The sediments consist of mixed carbonate-volcaniclastic packages with significant rhodolith accumulations. The aim of this study is to reconstruct the paleoenvironmental conditions under which the rhodolith accumulation was deposited and buried within an active volcanic setting.

Location and geological setting

The Azores Archipelago (Fig. 1) is located in the northeast Atlantic Ocean about 1400 km off the Portuguese mainland. The archipelago comprises a group of volcanic islands straddling the junction between three tectonic plates: the North American, the African (Nubian) and the Eurasian plates (França et al. 2003). Santa Maria is the oldest and the easternmost island, dating back to the late Miocene (Serralheiro et al. 1987; Serralheiro and Madeira 1990; Serralheiro 2003; Ramalho et al. 2014; Sibrant et al. 2015). It is the only island in the archipelago that preserves a rich fossiliferous sequence of Neogene sediments (Ferreira 1955; Zbyszewski and Ferreira 1962; Ávila et al. 2009, 2015b; Madeira et al. 2007), due to a fortuitous combination of volcanism, sedimentation, uplift and coastal erosion.

The volcanostratigraphic sequence of Santa Maria was described in detail by Serralheiro et al. (1987), Serralheiro and Madeira (1990) and Serralheiro (2003). The island first emerged during the late Miocene at around 6 Ma (Ramalho et al. 2014), during which time the Cabrestantes and Porto formations were deposited. Subsequently, an island formed as a shield (Anjos Complex), was largely eroded again during the latest Miocene and early Pliocene. During this phase, the existing island disappeared and became a guyot (Ávila et al. 2012), possibly with just a few islets emerging above water; contemporaneously, a large amount of volcaniclastic and bioclastic sediments, interfingering with synchronous low-volume submarine lava flows, was deposited (Touril Complex). During the early Pliocene, volcanic activity increased again, gradually raising the island again above sea level (Facho-Pico Alto Complex). In the late Pliocene and Pleistocene, erosion and uplift again prevailed, combined with low-volume volcanism during the late Pliocene (Feteiras Formation).

The Malbusca locality features a ~150-m plunging cliff that exposes the edifice's volcanostratigraphic sequence at its southernmost point. The sequence corresponds to a subhorizontal stack of basaltic submarine lava flows interbedded with less voluminous fossiliferous marine sediments, capped by subaerial lava flows and a small cinder cone (Fig. 1). The base of the sequence, comprising the first set of submarine flows and the first (thicker) package of marine sediments was considered as part of the Touril Complex by Serralheiro et al. (1987), which can be traced intermittently along the south and western side of the island to the north shore. Therefore, within this context, the sedimentary sequence reflects a period in which the island edifice resembled a shallow, sandy bank where marine life thrived. The overlying submarine products, minor marine sedimentary layers, and capping subaerial products were considered as part of the Facho-Pico Alto Complex. A recent work by Sibrant et al. (2015) dated the lava flows below and above the main (lower) sedimentary package—the focus of this study—yielding 4.32 ± 0.06 and 4.02 ± 0.06 Ma, respectively; Sibrant et al. (2015), however, erroneously described the upper flow as subaerial when in fact it is a submarine sheet flow. Their study nevertheless provides a well-constrained age for the sedimentary sequence that is the focus

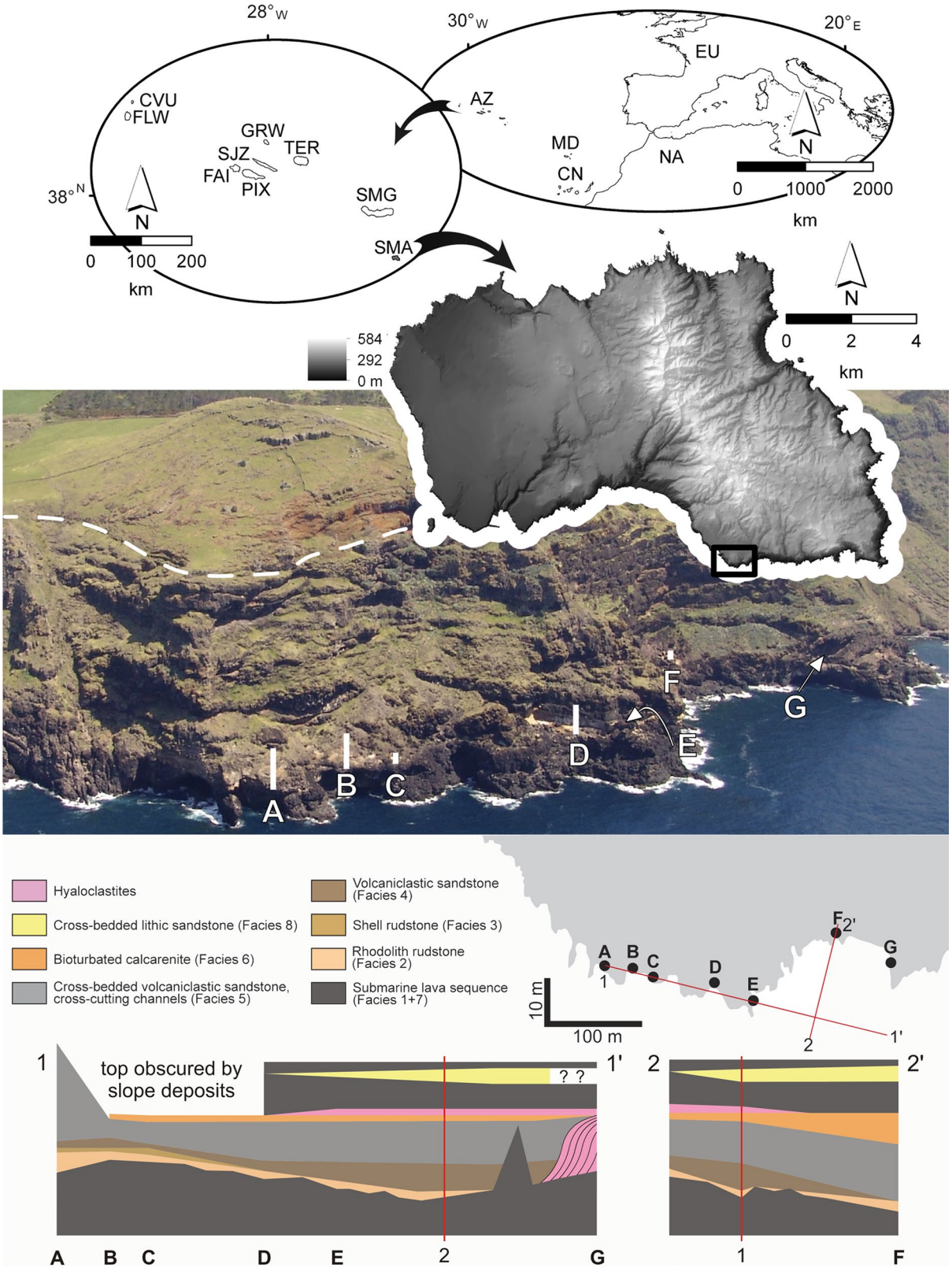

Fig. 1 Location of the Azores Archipelago with respect to Santa Maria Island and the outcrop studied: *A–G* location of the logs studied; *white dashed line* marks the passage zone between submarine units and subaerial units; and model of the spatial relationship of the sedimentary units exposed at the Malbusca section, based on the correlation of the individual logs and field data. Note strong relief of underlying pillow lavas, hyaloclastite foresets in the east, and thickening of the sedimentary succession towards the north. Height of sections exaggerated by a factor of five

of this study, safely placing it in the early Pliocene and not the late Miocene, as it has been previously suggested.

Methods

To capture the full diversity of the laterally rapidly changing facies, five stratigraphic logs were compiled at various intervals along the studied outcrop. These are, from west to east: Malbusca A–D and F (Fig. 1). Two other sites (Malbusca E, G; Fig. 1) were used to complement facies lateral variation, but were not studied in detail. The rhodolith layer was separated into different units according to the recognized beddings.

Growth forms of rhodoliths, additional biological encrustations and borings were registered in the field. Whole rhodolith specimens from stratigraphic levels near the base of the succession above the unconformity were collected at two localities and measured (to the nearest millimeter) across three principal axes (long, intermediate, and short). Data from these measurements were divided into spherical, ellipsoidal, and discoidal shapes according to the triangular diagram applied to rhodoliths by Bosence (1976, 1983). In addition, the rhodoliths from these collections were mechanically broken apart in order to determine the nature of their nuclei. Growth-form terminology follows Woelkerling et al. (1993).

A bulk sample (1–2 kg) containing several rhodoliths was taken from each bed (logs A–D) in order to study the taxonomy and sediment composition. Microfacies analysis and species relative abundance were appraised on the basis of 16 rhodolith thin-sections of 4.8 × 9.6 cm and 8 of 4.8 × 4.8 cm from the bulk samples. The quantification of thin-section components was conducted using estimation charts as described by Flügel (2004). All rhodolith samples are stored in the Fossil Collection of the Department of Biology at the University of Azores, under the acronym DBUA-F1084 to 1106.

Invertebrates were identified in the field or later in the laboratory. Sets of three samples (triplets) for calcareous nannofossil screening were collected at three distinct levels of Malbusca B and at five levels of Malbusca D of the described stratigraphic sections. The aim was to study the variability and the main overall parameters (quantity and diversity) of the coccolith assemblages. Due to the coarseness of the samples subsequent laboratorial preparation followed procedures described in Johnson et al. (2012). Calcareous nannofossils were identified by polarizing light microscopy at 1250× magnification.

Results

Stratigraphic logs

The location of the five stratigraphic logs performed during the course of this study, A–D and F, is shown in an aerial view of the Malbusca cliffs (Fig. 1). In this section, pillow lavas (facies 1; cf. Fig. 2) are overlain by sediments composed of rhodoliths in rock-forming quantities, as well as local patches with conglomerates and breccias formed by volcaniclastics. The sedimentary deposits are more or less continuously exposed for a lateral distance of 400 m and are situated about 20 m above present sea level. To the east, the outcrop can be traced along a ledge formed by the underlying volcanic rock, across a steep, inaccessible slope (E in Fig. 1) partly covered by fallen blocks and vegetation. Further east the strata are exposed again for a short stretch (F in Fig. 1), before onlapping against prograding foresets of hyaloclastites, preserved as part of an old lava delta (G in Figs. 1, 3a). There are no further outcrops at this level towards the east. In the west, in contrast, the Neogene sediments can be traced for approximately 2 km, but cropping out high up in the cliffs (rising up to more than 50 m above present sea level), being either inaccessible or completely covered by debris and vegetation.

The Neogene sediments rest on an eroded surface formed by pillow lavas with a topographic relief that varies laterally from 0 to 8 m. Locally, small volcanic pebbles are encrusted by biota and trapped within depressions (log A, Fig. 2). The topographic relief is filled up by a rhodolith rudstone that is laterally consistent through logs A to D. In some places, the rhodolith rudstone penetrates deeply in the underlying rock, filling fissures and crevices 1–2 m below the surface. Locally (logs A, C, E, and F) large basalt boulders lie at the base of the sedimentary succession. Sandstone follows unconformably above the rhodolith beds, containing local accumulations of shells and lithoclasts (both of volcanic and bioclastic origin) at the base. Unconformably above the sandstone follows a thicker unit of sandstones with hummocky cross-stratification and again larger bio- and lithoclasts at the base. The top part of the sedimentary succession is heavily bioturbated. The section is capped by a laterally extensive submarine sheet lava flow followed by a succession of more massive submarine sheet flows and pillow lavas. In the easternmost part of the outcrop, where the lava flow capping the underlying sediments is thicker, another layer of sediment that pinches out towards the west is intercalated within the lava (Fig. 2, log F) (for a summary of the different facies see Table 1).

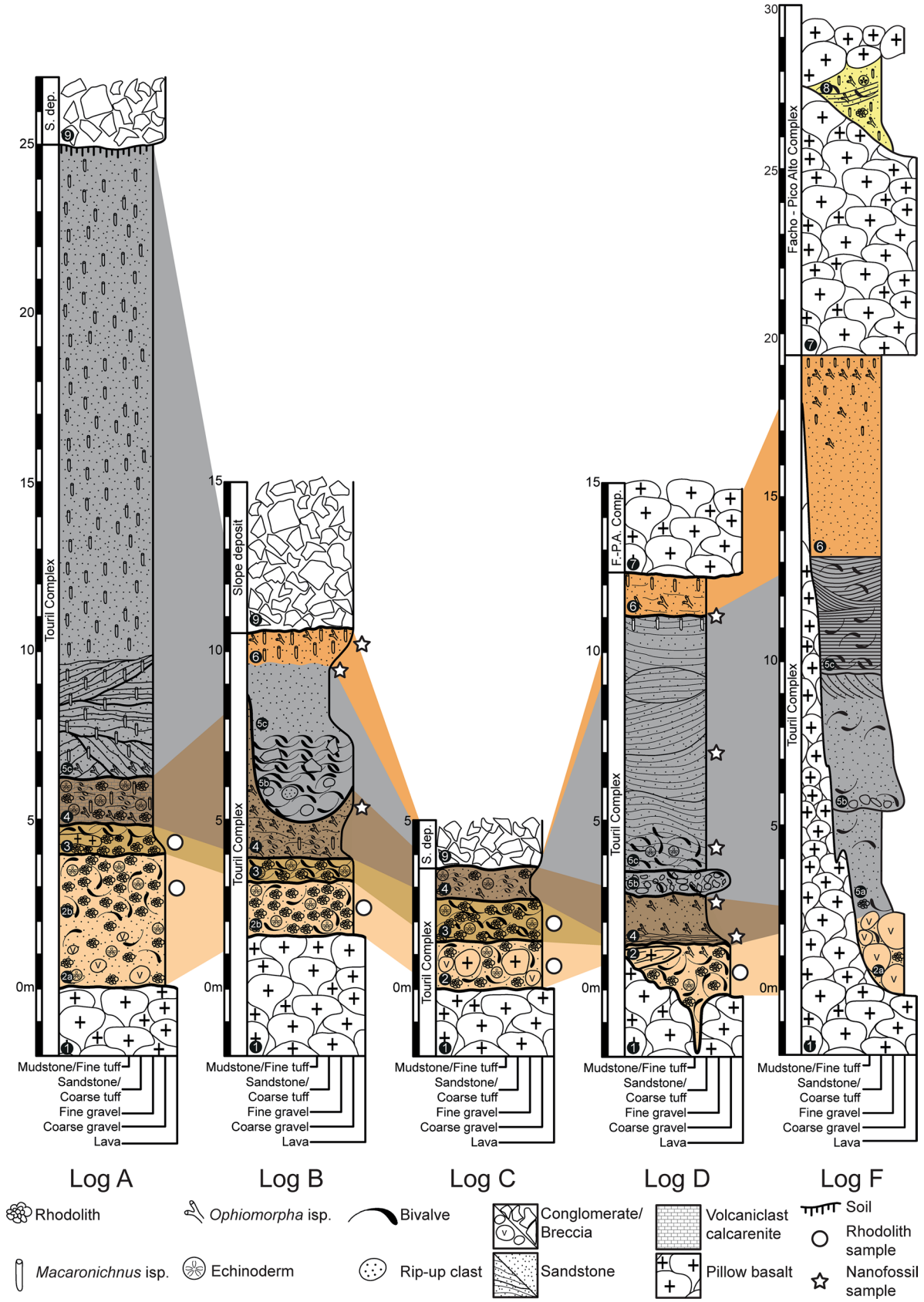

Fig. 2 Detailed stratigraphic logs from the Neogene sequence at Malbusca, with correlation of the different lithofacies across the different logs. *Star* and *circle symbols* indicate respectively the collecting location for calcareous nannofossils and rhodoliths

Table 1 Summary description of distinguished facies and their interpretation

	Description	Interpretation	
Facies 1	Pillow lava	In situ pillow lava forming topographic relief	
Facies 2a	Sandstone, mainly calcarenitic	Multiphase tempestite(s)	Finer-grained sediment trapped within the relief
Facies 2b	Rhodolith rudstone		Mixture of in-situ and transported rhodoliths
Facies 3	Shell rudstone or shell breccia		Reworked shells after storms
Facies 4	Bioturbated volcaniclastic calcarenite/sandstone		Decrease of hydrodynamic energy compared to facies 3
Facies 5a + b	Coarse bioclastic/volcaniclastic sandstones with bioturbation on top		Filling of accommodation space with shallow subtidal traces at the top
Facies 5c	Coarse bioclastic/volcaniclastic sandstones with hummocky cross-stratification		Storm deposit after time of quiescence represented by burrowing on top of 5b
Facies 6	Sandstone bioturbated to varying degrees		Shallow subtidal
Facies 7	Pillow lava	Lava flow terminating the sedimentary succession	
Facies 8	Cross-bedded sandstone	High-energetic intercalation within submarine lava flows	
Facies 9	Breccia	slope deposit	

Malbusca log A

Malbusca log A starts with a 2-m-thick sandstone unit (facies 2a in Figs. 2, 3b) rich in bioclasts, including shells of *Spondylus gaederopus*, *Ostrea* spp., various pectinids, other bivalve shell debris, subordinate echinoid tests of *Eucidaris tribuloides* and *Clypeaster altus* as well as fragments of the balanid *Zullobalanus santamariaensis*. At the base, basalt cobbles of up to 20 cm occur. Basalt pebbles (2–4 cm in diameter) and rhodoliths are common within the whole unit. In the upper part, some of the rhodoliths show volcanogenic nuclei. The transition to the following unit is gradual and mainly related to an increase in rhodolith abundance and vanishing of lithoclasts.

Above follows a ca. 2-m-thick dense rhodolith accumulation (rhodolith rudstone, facies 2b, Fig. 2), composed mainly of rhodoliths ranging from 2 to 3 cm in diameter. Rhodolith nuclei, when visible, are represented by bivalve shell fragments; growth forms range from encrusting to lumpy, with some warty rhodoliths in the top part of the

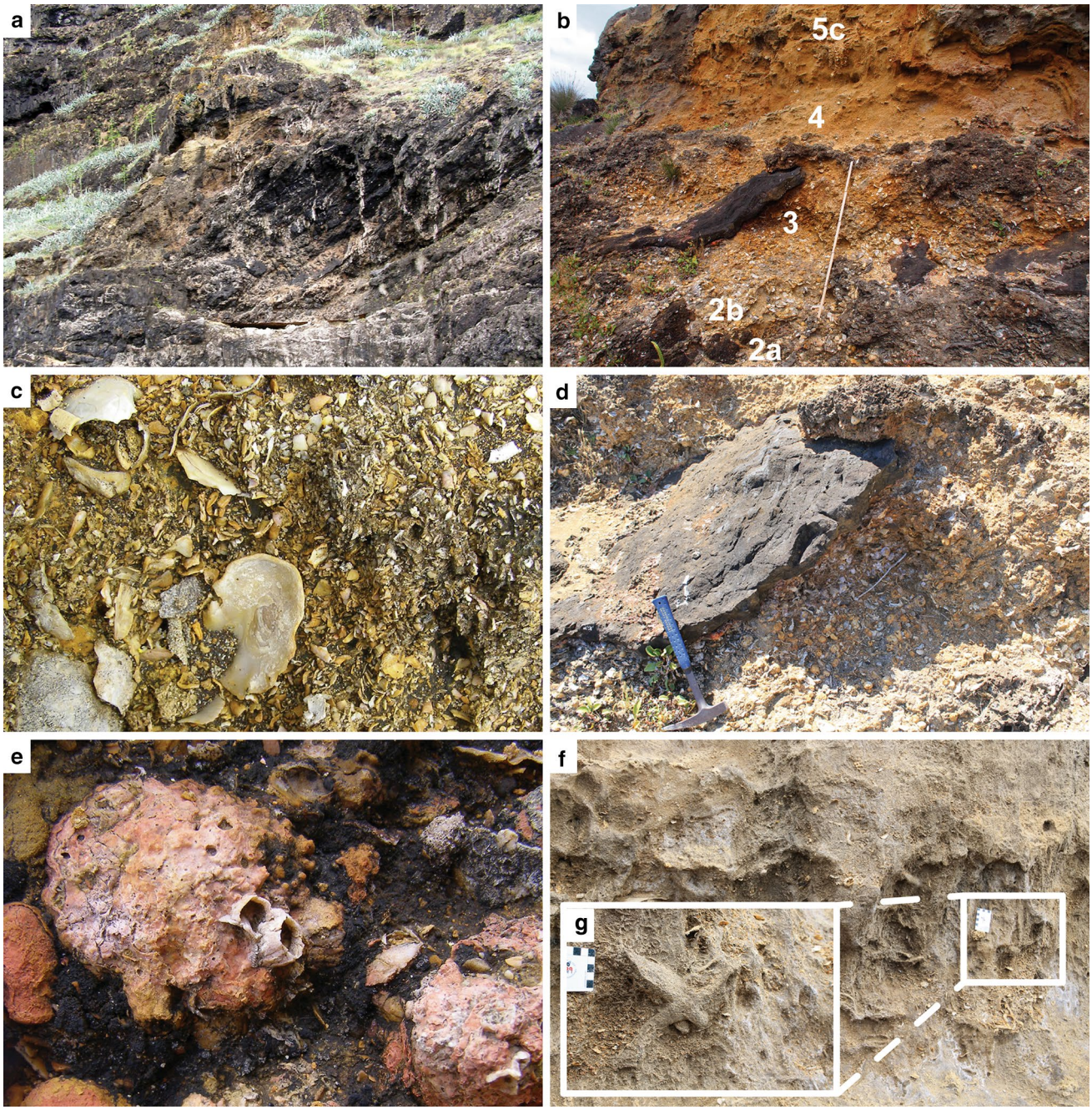

Fig. 3 **a** Hyaloclastite foresets (position G in Fig. 1). **b–g** Views of Malbusca A with details of the different units. **b** Overview of Malbusca A. **c** Shell rudstone (log A; *scale bar* equals 1 cm). **d** Detail of the basal rhodolith rudstone with magmatic intrusion. **e** Rhodolith overgrown by barnacles from top of the rhodolith rudstone (log A; *scale bar* equals 1 cm). **f** Bioturbated sandstone unit (facies 5c). **g** Detail of facies 5c, where it is possible to see trace fossils of different sizes (smaller *Macaronichnus segregatis* and larger *Thalassinoides* isp.)

bed. Rhodoliths are mostly spheroidal and ellipsoidal in outline. Again, bivalve debris is abundant, while echinoderm fragments occur less commonly.

Facies 3 is a shell rudstone or shell breccia with a thickness of 80 cm (Fig. 3c). Shells are mostly fragmented, disarticulated and do not show preferred orientation. Bivalve shells belong to oysters, pectinids and spondylids (see "Appendix"). Most shells and some rhodoliths are bioeroded (mostly *Entobia* isp. produced by clionid sponges and *Gastrochaenolites* isp. produced by the endolithic

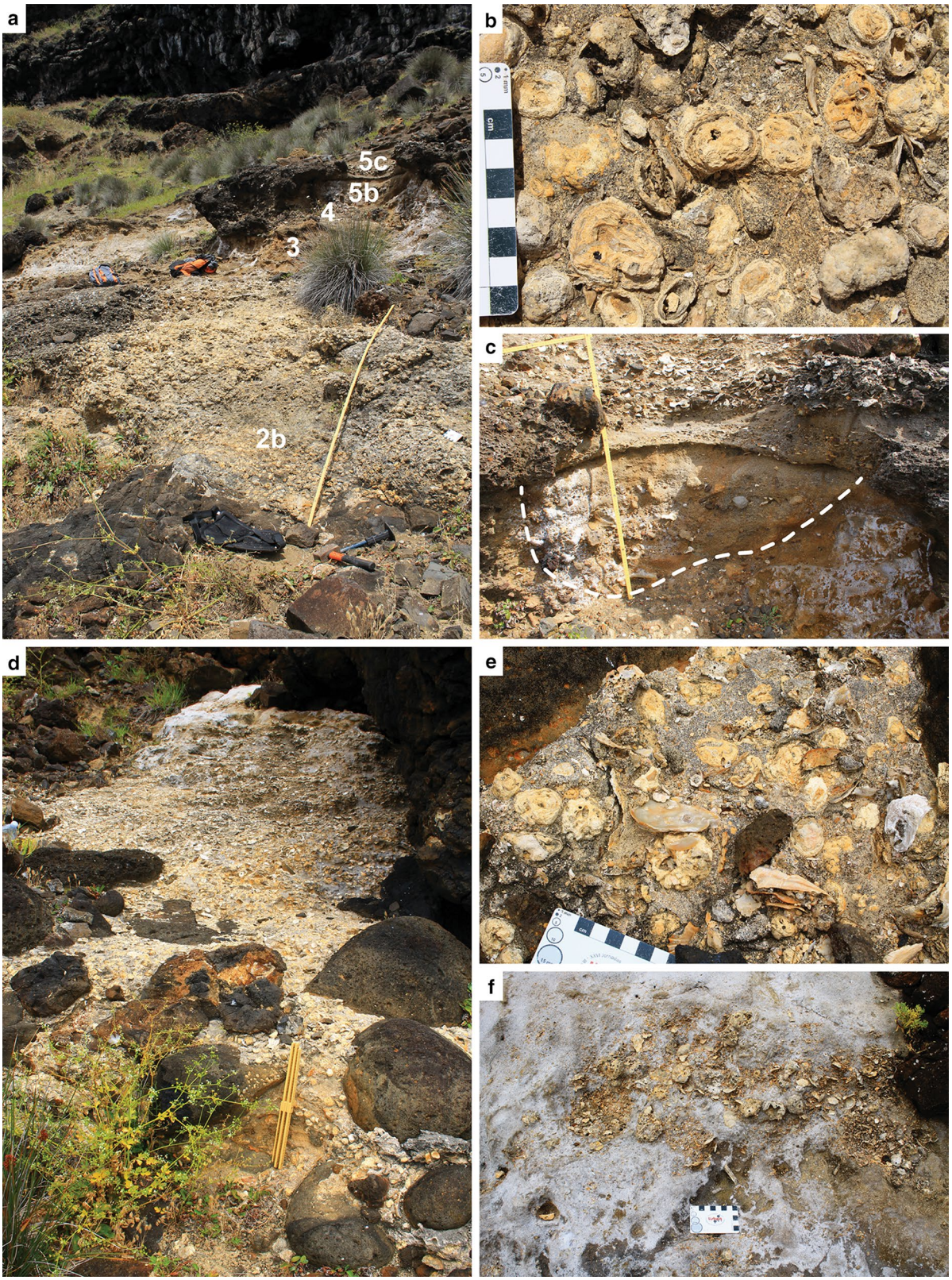

Fig. 4 Views of Malbusca B and C with details of the different units. **a** Overview of Malbusca B. **b** Detail of the basal rhodolith rudstone unit. **c** Detail of the multiphase filling channel unit. **d** Overview of Malbusca C. **e** Detail of the basal rhodolith rudstone unit. **f** Detail of the sandstone with patches of rhodoliths and shells

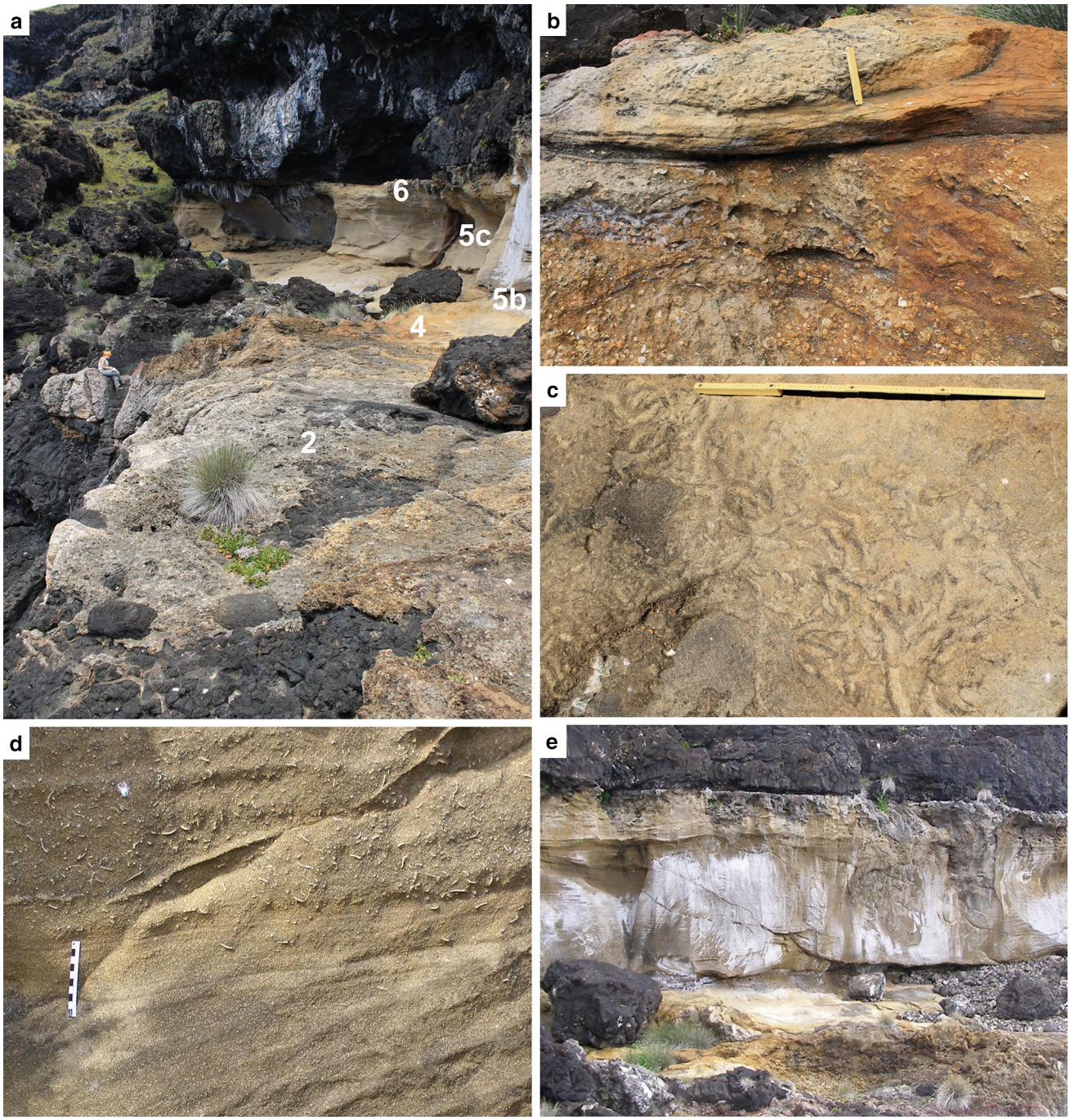

Fig. 5 Views of Malbusca D with details of the different units. **a** Overview of Malbusca D (person for scale). **b** Detail of the basal rhodolith rudstone and bedded sandstone. **c** Detail of the bioturbational structures (?*Bichordites* isp.) on top of the 20-cm bedded sandstone. **d** Transition from facies 5 to 6, with onset of abundant *Macaronichnus* isp. (log D; scale is 10 cm long). **e** Succession of log D, note planar top of bioturbated calcarenites (facies 6) overlain by a submarine lava flow

bivalve *Myoforceps aristatus*). A magmatic layer seems to be intruding into the sediment (Fig. 3d). This facies type is present in Malbusca A, B, and C.

Above, 1.5 m of volcaniclastic calcarenites follow (facies 4). These sediments are strongly bioturbated, but locally remnants of cross lamination and bedding is present. Centimeter-sized shell and echinoid fragments are accumulated in patches. Rhodoliths of 4–8 cm diameter occur, some of which are encrusted by the barnacle *Z. santamariaensis* (Fig. 3e). The calcarenites are partly bioturbated. Trace fossils are represented by large, variably oriented, branched, tubular burrows, mostly 1.5–3 cm in

diameter, including unlined *Thalassinoides* isp. and lined *Ophiomorpha* isp. (Fig. 3f, g), small, mostly vertical burrows, 2–3 mm in diameter, lined with darker, volcaniclastic grains (*Macaronichnus segregatis*) and variably oriented, slightly winding, smooth tubes, 7–10 mm in diameter (*Palaeophycus* isp.). Less common trace fossils are represented by (1) a large oblique cylinder without wall, 40–45 mm in diameter (?*Psilonichnus* isp.), which occurs in the lowest part of this facies; (2) vertical tubes, 30 mm in diameter, lined with shell fragments (*Diopatrichnus* isp.); and (3) bowl-like depressions, about 20 cm wide and 5 cm deep (*Piscichnus* isp.).

Facies 4 is overlain by 5c in log A, while 5a and 5b are missing here. It is ~20 m thick and incompletely exposed in log A, the upper part of which is covered by vegetation and rockfall. The lower 3–4 m of this unit consist of coarse bioclastic/volcaniclastic sandstones with hummocky cross-stratification. Bioclasts are scarce, but trace fossils are abundant, involving large branching, tubular burrows (*Ophiomorpha* isp.), smaller (7–10 mm in diameter), unbranched, horizontal ones (*Palaeophycus* isp.), and irregular, small, tubular burrows lined with dark grains (*M. segregatis*). A horizon with horizontal, winding, tubular, back-filled structures, 20–25 mm wide (*Bichordites* isp.) is present about 5 m from the base of this facies. The sediments are totally bioturbated except for local remnants of small-scale cross bedding.

Malbusca log B

In contrast to log A, the succession starts with 1.7 m of rhodolith rudstone (facies 2b) lying directly on top of the eroded pillow lavas (Fig. 4a). Facies 3, the shell rudstone, reaches only 60 cm in log B. Owing to its increased content of volcaniclastic material it is darker than the underlying rhodolith rudstone (Fig. 4b). Again bioturbated sandstones (facies 4) follow above, but cross bedding is even less distinct than in log A. The thickness of this bed varies from 3.8 in the west to 2.0 m in the east, due to the existence of a palaeo-channel (Fig. 4c). The channel is 1.8 m deep and shows a multiphase filling (facies 5b) of coarse bioclasts (mainly bivalve shell fragments encrusted by bryozoans), rip-up clasts at the base, and a mixture of shell debris and basalt lithoclasts. The latter include both angular (up to 7 cm) and rounded lithoclasts (1–5 cm). Large oyster and pectinid shells, mostly fragmented and bioeroded, occur. The matrix between the larger clasts is a coarse sandstone similar to the unit above (facies 5c, 3 m thick), which here is less strongly bioturbated than in log A. On top of this follows another sandstone bed, ca. 1 m in thickness, that is intensively bioturbated (facies 6) with *Ophiomorpha* isp. and *Piscichnus* isp. (in the upper part), and *Macaronichnus* isp. (throughout the bed). The top of the sequence is covered by modern slope deposits.

Malbusca log C

Only the lowermost three units are exposed in log C (Fig. 4d). At the base, 1.4 m of rhodolith rudstone with basalt lithoclasts ranging from 5 cm to 1 m in diameter (usually well rounded) is exposed (Fig. 4e). The boulders are never encrusted, neither by coralline algae, nor by barnacles. Here facies 2a and 2b, which are quite distinct in log A, are amalgamated and cannot be well differentiated. Above follows 1.2 m of shell rudstone (facies 3) as in logs A and B, with abundant disarticulated bivalve shells (see "Appendix"), many of them encrusted by the barnacle *Z. santamariaensis*. Remains of the large echinoid *C. altus* are also visible. Thereafter, ca. 90 cm of bioturbated, volcaniclastic sandstones (facies 4) are exposed. Horizontal burrows dominate (?*Thalassinoides* isp.) and patches of rhodoliths and shells occur (Fig. 4f). Further to the east, the sandstones display *M. segregatis*, *Ophiomorpha* isp. and *Piscichnus* isp. The top of the section is covered by modern slope deposits.

Malbusca log D

Unlike the three more westerly logs, log D encompasses most of the sedimentary sequence of the Malbusca outcrop (Fig. 5a). The succession starts with up to 3 m of rhodolith rudstone (facies 2) filling the underlying relief. Locally, the unit penetrates 2 m into crevices in the basement. The matrix consists mainly of silt- to sand-sized bioclasts, whereas volcaniclastic material is subordinate (10–20 %). Rhodoliths are highly abundant, locally forming a grain-supported rudstone. In the middle of facies 2, the rhodoliths are preserved in 5-cm-thick layers that are distinctly cross-bedded. Higher up in facies 2, bivalve shells (pectinids, oysters, spondylids) appear usually in horizontal layers with a slight preference for convex-up orientation. Rhodolith size ranges from 2 to 6 cm in diameter (Fig. 5b) and nuclei, where visible, include shell fragments and rare basaltic lithoclasts. Some rhodoliths show incrustations by balanids (*Z. santamariaensis*), but these are restricted to the outer surface. Moulds of dissolved large gastropods (strombids) occur occasionally, but as a rule, most aragonitic molluscs are completely dissolved. Likewise, echinoid remains (*Eucidaris* spines, *C. altus* fragments) commonly occur. The uppermost 30 cm of the unit contain fewer rhodoliths and shells, but *M. segregatis* and poorly preserved *Ophiomorpha* isp. are present. Above these, a 1.5-m-thick unit of heavily bioturbated volcaniclastic packstones follows (facies 4). Locally, a laminated layer, 15 cm thick (Fig. 5b) cuts erosively into the upper part of the rudstone (facies 2). It is covered by a thin (20 cm), laterally

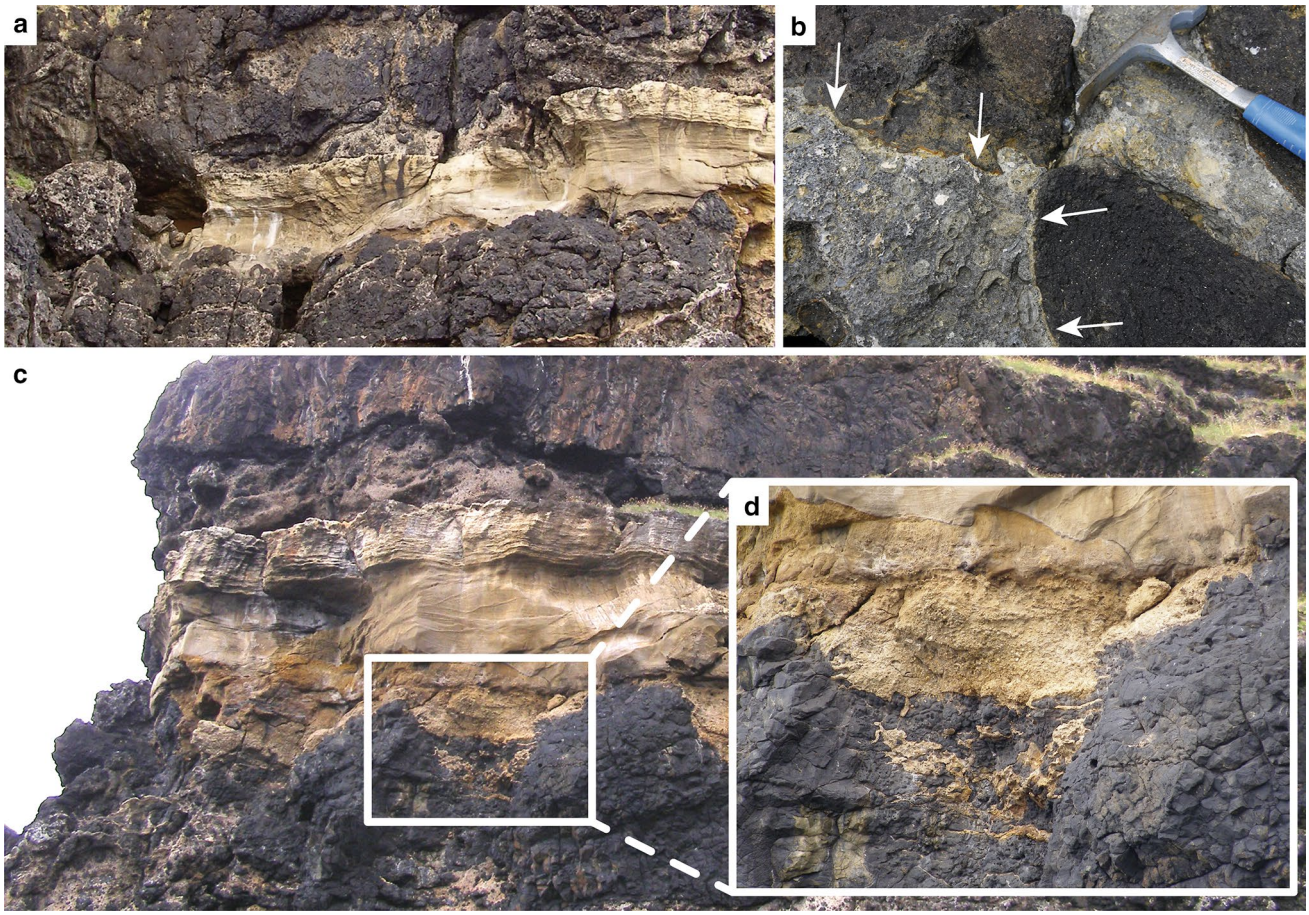

Fig. 6 Complete sedimentary succession about 7 m thick exposed in the vertical walls of a narrow rock spur projecting from the cliffs at position "E" in Fig. 1. **a** The rhodolith rudstone is poorly developed on the western side. **b** Large cobbles at the base of the sequence encrusted by platy coralline algae (*arrows*). **c** the rhodolith rudstone fills the deeper relief on the eastern side; Towards the north (*right* in **c**) the rhodolith rudstone pinches out. **d** Detail of rhodolith rudstone infilling relief of basement (log E). Towards the south (*left* in **c**) a layer of hyaloclastites is wedged between the top sedimentary bed (bioturbated calcarenite, facies 6) and the overlying lava flow. Note the different thickness of the individual beds on the western (**a**) and eastern (**c**) side of this cliff

discontinuous layer of coarse sandstone. It is intensively bioturbated with *Bichordites* isp. (Fig. 5c). Above, the sandstones (facies 5b) are intensively bioturbated (*M. segregatis*, *Ophiomorpha* isp., *Piscichnus waitemata*), and contain one 80 cm in thick horizon with *Bichordites* isp. in the center).

The overlying unit (facies 5c) again erosively cuts into the underlying one. It is a 0.5–6-m-thick bed of sandstone, similar in grain size to the unit below, but with much higher content of volcaniclastic material (close to 80 %). It is weakly cross-stratified and contains numerous basaltic lithoclasts (up to 6 cm in diameter, both rounded and angular ones) and intraclasts (up to 18 cm) at its base. Originally aragonitic bivalves seem to have been very abundant, but they are completely leached, leaving indistinct moulds. On top of this, a rich fossiliferous layer (up to 1.2 m thick) that contains mollusc shells (oysters and pectinids) and echinoid fragments (tests of *Clypeaster* and *Echinocyamus*, *Eucidaris* spines), as well as moulds of large gastropods (strombids) and intraclasts (up to 10 cm), occurs embedded within a volcaniclastic sandstone. The top part of the bed contains *M. segregatis* which is usually concentrated in proximity of sparse, branched *Ophiomorpha* isp. (it descends up to 1.5 m down from the top), and *Palaeophycus* isp.

Above, a 1.6–2-m-thick series of hummocky cross-stratification or planar sandy calcarenite beds occur (facies 6; Fig. 5d). Bases of the beds are locally channelized. The beds do not contain macrofossils and are partly bioturbated. The top of the series of beds is planar and capped by a layer of basalt with the typical entablature jointing of submarine sheet flows, exhibiting small-scale peperites at the base (Fig. 5e).

Malbusca log E

Approximately 40 m to the ESE of log D, the cliff forms a point with near-vertical sides that exposes a sedimentary sequence. While the upper cliffs are not accessible for

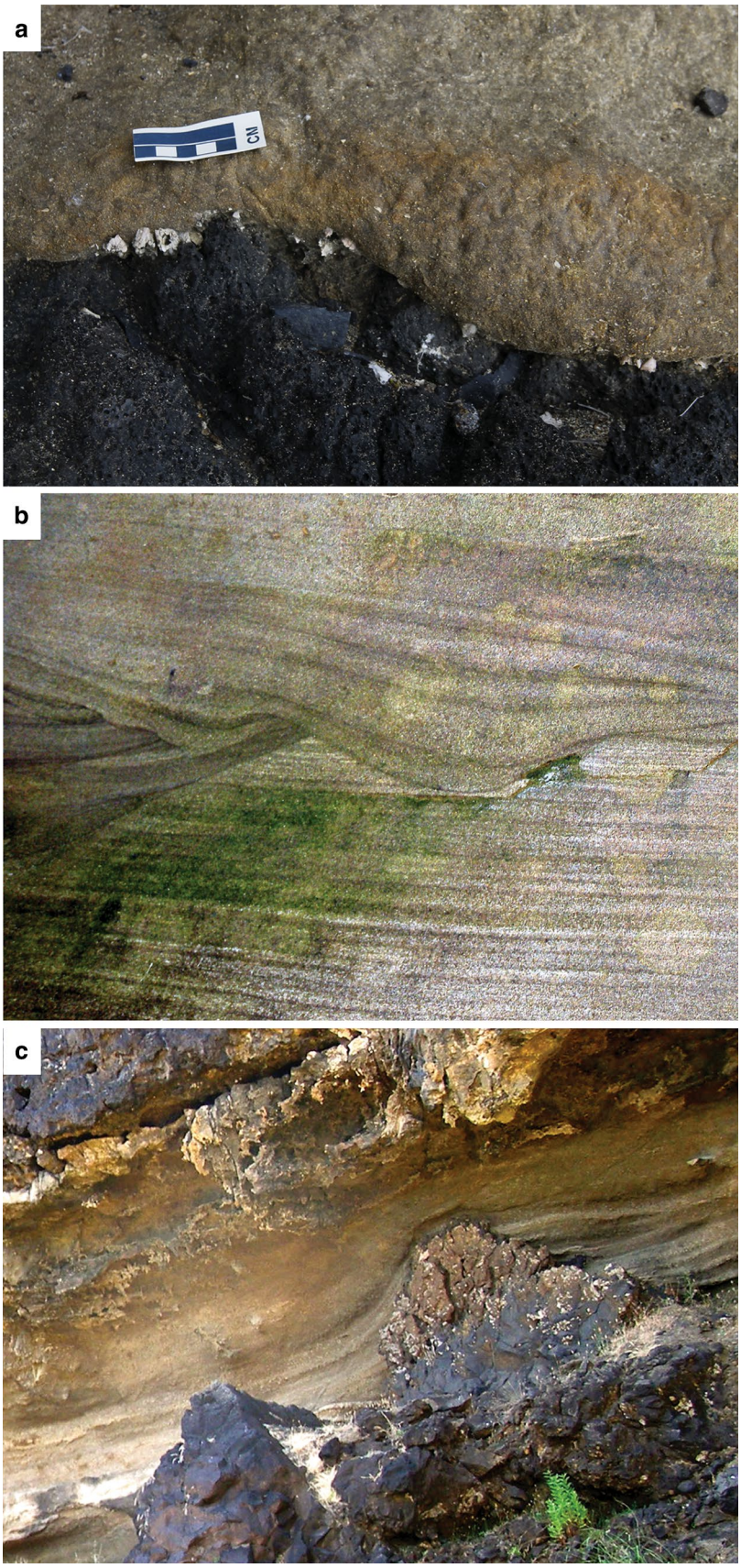

Fig. 7 Sedimentary features of the Malbusca succession. **a** Top surface of basalt pillows encrusted by barnacles. **b** Cross-bedding in facies 5c (log F, meter 12). **c** Onlap of sedimentary units on basement protrusion (*top* of log F)

detailed logging, the section provides excellent insights into the spatial relationship of the different sedimentary units from the distance. The topographic relief of the underlying pillow-basalt is very pronounced (Fig. 6a). Large cobbles deposited within the topographic saddles are encrusted by platy coralline red algae (Fig. 6b). On the southernmost point, a wedge of hyaloclastites with occasional pillows is interspersed between the topmost sediment layer (facies 6) and the overlying submarine sheet flow, which becomes thicker towards the south (Fig. 6c). In addition, it shows that the rhodolith accumulation pinches out towards the north (Fig. 6d), and that the sandstone units of facies 4 and 5 rest directly on basement rocks.

Malbusca log F

The eastern- and northernmost outcrop of the Malbusca section exposes a ca. 50-m-wide depression within the basement filled by a thick sedimentary package. At the eastern end of the outcrop, where the basement rises high up, the top surfaces of some basalt pillows are encrusted by barnacles (Fig. 7a). In the center of the depression, a 2.5-m-thick basal conglomerate is exposed, containing well-rounded cobbles and boulders between 5 cm and 2.5 m in diameter. The matrix in between is a fine-grained volcaniclastic packstone with poorly preserved moulds of aragonitic molluscs, pectinids, oysters, *Eucidaris* spines and few rhodoliths (facies 2a). Above, a ~2.9-m-thick lithic packstone to bioclastic sandstone follows, locally with indistinct bedding and traces of mollusc moulds (facies 5a). The next unit comprises 4 m of lithic coarse sandstone containing well-rounded basalt pebbles (5 mm to 10 cm in diameter) at the base. Indistinct bedding caused by repetitive cycles of normal grading can be observed, which seem to be the result of successive events. Towards the top, the content of biogenic material increases and indistinct mollusc moulds and cross-bedding occur. Laterally, the beds show onlap onto the basaltic basement (facies 5b). At the top, another unit of coarse lithic sandstone follows (3.8 m thick), being characterized by cm-size bedding or grading revealed by differential weathering. It is extremely rich in mollusc shells and their shell fragments, most of which are completely leached and preserved as moulds. Locally, lamination is visible and internal bedding is common (facies 5c; Fig. 7b). The top of this unit is truncated albeit being more or less planar, and is followed by ca. 6 m of lithic sandstones with 20–50 cm foresets propagating in a westerly direction. Fossils are rare and restricted to small shell fragments floating in the matrix. The uppermost 2 m of the unit are strongly bioturbated. The top of the bed is planar, slightly inclined towards the NW and covered by a massive (ca. 10 m) basaltic submarine sheet flow (facies 7) (Fig. 7c). Above this lava flow, another bed of cross-bedded lithic sandstone is visible. It is thickest in the east (3 m) and pinches out towards the west. Fossils are common, consisting mainly of molluscs (pectinids, oysters, spondylids) and *Eucidaris* spines. Rhodoliths and rounded basalt pebbles (5–10 cm in diameter) are rare (facies 8). This bed is again overlain by basaltic submarine sheet flows, which, in alternation with pillow lavas, continue to the top of the cliffs, where the sequence is overlapped by subaerial volcanic products.

Sedimentary components and bioclasts

Bulk samples collected from the rhodolith rudstone in logs A to D were studied through thin-sections. The biogenic components are dominated by coralline red algae, peyssonneliacean algae, foraminifera, bryozoans (both erect and encrusting forms), bivalves, barnacles and fragments of echinoderms. The distribution of the different taxa in the studied facies and logs is listed in the "Appendix".

Volcaniclastic component

The volcaniclastic sediment component is dominated by basaltic lithoclasts and mineroclasts of diverse nature (olivine, clinopyroxene, plagioclase). Secondary magnetite can be found widespread both in the biogenic component and the basaltic lithoclasts. Sparitic cement fills the pores.

Basaltic lithoclasts are rounded with a variable degree of weathering. The largest grains (1.5 mm) are less weathered. The texture of these clasts is porphyritic with a seriate matrix. The mineral assemblage is typical of basalts, being formed by acicular plagioclase, olivine and clinopyroxenes. The smaller lithoclasts are completely weathered and oxidized. Loose crystals are either subangular or rounded fragments of mafic phases with typical sizes ranging between 150 and 700 µm. In order of rank abundance, they occur as clinopyroxenes and olivines, followed by plagioclases.

Coralline algae

Coralline algae are represented by encrusting non-geniculate taxa forming unattached nodules known as rhodoliths. These compose up to 33 % of the sediments, whereas their fragments compose up to 11 % (Table 2). The rhodoliths are multispecific and dominated by coralline algae [*Lithophyllum prototypum*, *Lithophyllum* sp., *Spongites* sp., *Hydrolithon* sp., *Phymatolithon calcareum* and cf. *Phymatolithon* sp. (for details on a full taxonomic classification see Rebelo et al. 2014)] intergrown with peyssonneliacean algae (*Polystrata alba*) and encrusting bryozoans. The transition from one species to the other is often marked by abrasion and borings by bivalves and or sponges (Fig. 8). For example, *P. calcareum* (number 7, Fig. 8) is most frequently encrusted by peyssonneliacean algae (number 12,

Table 2 Percentages of the biogenic and volcanic components for each bed of the four logs (A–D)

Rhodolith facies	All components (%)												
	Coralline algae			Echinoids		Foraminifera			Bryozoa		Barnacles	Molluscs	Volcanic clasts
	Rhodoliths	Fragments of geniculates	Frag. of non-geniculates	Spines	Test fragments	Textularids	Miliolids	Hyaline	Encrusting	Erect			
Malbusca A: facies 2b	19	3.2	6.5	6.5	0	6.5	6.5	13	6.5	13	3.2	3.2	13
Malbusca A: facies 3	18	2.9	5.9	5.9	12	5.9	5.9	5.9	0	5.9	18	2.9	12
Mal. B: fa. 2b (first 40 cm)	21	5.3	11	5.3	11	5.3	5.3	16	0	5.3	2.6	2.6	11
Mal. B: fa. 2b (first 40 cm)	27	2.7	11	5.4	5.4	5.4	5.4	16	0	5.4	5.4	2.7	8.1
Mal. B: facies 2b (80 cm)	33	2.7	5.5	5.5	11	5.5	5.5	16	0	5.5	2.7	2.7	4.1
Mal. B: facies 2b (120 cm)	32	2.7	5.3	5.3	11	5.3	5.3	16	0	5.3	5.3	2.7	4
Mal. B: facies 2b (140 cm)	23	2.9	5.7	5.7	5.7	11	5.7	11	0	11	5.7	2.9	8.6
Mal. B: facies 2b (155 cm)	29	2.9	5.7	5.7	5.7	11	5.7	11	0	5.7	5.7	2.9	8.6
Mal. B: facies 2b (170 cm)	8	4	4	8	8	8	0	8	8	16	8	4	16
Mal. C: fa. 2 (first 40 cm)	27	3.3	3.3	6.7	6.7	6.7	6.7	6.7	6.7	6.7	6.7	3.3	10
Mal. C: facies 2 (80 cm)	7.7	3.8	7.7	7.7	7.7	7.7	0	7.7	7.7	7.7	15	3.8	15
Mal. C: facies 2 (120 cm)	24	3	6.1	6.1	6.1	6.1	0	12	6.1	6.1	12	3	9.1
Mal. C: facies 3 (160 cm)	24	0	4	0	8	8	0	8	8	8	16	4	12
Mal. C: facies 3 (200 cm)	22	3.7	7.4	7.4	7.4	7.4	7.4	7.4	0	0	15	3.7	11
Mal. C: facies 3 (200 cm)	24	2.9	5.9	5.9	5.9	5.9	5.9	12	5.9	0	12	2.9	12
Mal. C: facies 3 (240 cm)	13	3.3	6.7	6.7	6.7	6.7	6.7	13	6.7	6.7	6.7	3.3	13
Mal. C: facies 3 (280 cm)	8.3	4.2	4.2	8.3	8.3	8.3	8.3	8.3	8.3	8.3	4.2	4.2	17

Table 2 continued

Rhodolith facies	All components (%)												
	Coralline algae			Echinoids		Foraminifera			Bryozoa		Barnacles	Molluscs	Volcanic clasts
	Rhodoliths	Fragments of geniculates	Frag. of non-geniculates	Spines	Test fragments	Textularids	Miliolids	Hyaline	Encrusting	Erect			
Mal. D: fa. 2 (first 25 cm)	8.5	4.3	8.5	8.5	8.5	8.5	8.5	8.5	0	8.5	17	4.3	6.4
Mal. D: facies 2 (40 cm)	0	5.4	11	11	11	11	11	11	0	11	5.4	5.4	8.1
Mal. D: facies 2 (60 cm)	18	6	12	6	6	12	6	18	0	6	3	3	4.5
Mal. D: facies 2 (31 cm)	16	5.3	11	5.3	5.3	11	5.3	16	5.3	11	5.3	2.7	1.6
Mal. D: facies 2 (31 cm)	12	6.2	6.2	6.2	6.2	12	6.2	12	6.2	6.2	12	3.1	4.6
Mal. D: facies 2 (94 cm)	11	5.3	11	5.3	5.3	11	5.3	11	5.3	11	11	2.6	7.9
Mal. D: facies 2 (129 cm)	0	7	14	7	7	14	7	14	7	7	7	3.5	5.3
Total (mean)	19	3.9	7.5	6.1	7.2	8.3	5.3	12	3.5	7.2	8.3	3.v2	8.9

Fig. 8), or by bryozoans (number 17, Fig. 8), or its surface is abraded (number 14, Fig. 8). However, a general growth-succession trend was not observed.

In all sections, fragments of geniculate coralline algae are present in the sediments, contributing up to 3.9 % (see Table 2). No further identification was possible due to the fragmentary preservation of the material (Fig. 9a). The sedimentary matrix between the clast-supported rhodoliths is composed of bioclastic fragments derived from molluscs, sea urchins, barnacles, foraminifera, rhodolith debris and volcanic clasts.

The rhodoliths are mostly non-nucleated, with rare shells or volcaniclasts as nuclei. Also smaller and abraded rhodoliths can serve as nuclei for new rhodoliths (Fig. 9b). Some of the rhodoliths are completely bored by the bivalve *M. aristatus*. This led to the dissolution of the core, allowing it to be filled by the surrounding sediment (Fig. 9c, e, f). The bivalve borings (*Gastrochaenolites* isp.) are partially or completely filled with sediment that does not always correspond with the surrounding matrix of the rhodolith rudstone (Fig. 9c–e).

Measurements in the field revealed that rhodoliths have maximum diameters between 2 and 8 cm. Size and shape

Fig. 9 Rhodoliths and thin-section components. **a** Fragments of geniculate coralline algae (thin-section: Malbusca D, facies 2). **b** Bored and abraded rhodolith serving as nucleus for another rhodolith (thin-section: Malbusca B, facies 2b). **c** Rhodolith with a dissolved nucleus filled with sediment (thin-section: Malbusca A, facies 2b). **d** Rhodolith with dissolved core filled by different sediment from the surrounding sediment, composed by coralline and peyssonneliacean algae (thin-section: Malbusca A, facies 2b). **e** Rhodolith nucleus dissolved and filled with a sediment different from the surrounding (thin-section: Malbusca B, facies 2b). **f** Non-nucleated multispecific rhodolith, borings filled by surrounding sediment, abrasion in between the different coralline taxa (thin-section: Malbusca B, facies 2b). **g** Thin crusts of coralline algae forming a box work rhodolith (thin-section: Malbusca C, facies 3). **h** Enrolled hyaline foraminifer (thin-section: Malbusca A, facies 2b). **i** Trochiform hyaline foraminifer (thin-section: Malbusca A, facies 2b)

of the rhodoliths is independent of the size and shape of the nuclei. The majority of the rhodoliths (89 %, $n = 25$) is laminar-concentric in shape. Only three rhodoliths (11 %) with different growth forms were found: laminar box work, branching to laminar box work (Fig. 9g), and columnar. A total of 32 and 41 whole rhodoliths were collected for measurements from the middle rhodolith bed of Malbusca sections B and D, respectively. The results are shown in the triangular diagram of Fig. 11. Rhodoliths of both sections are plotted

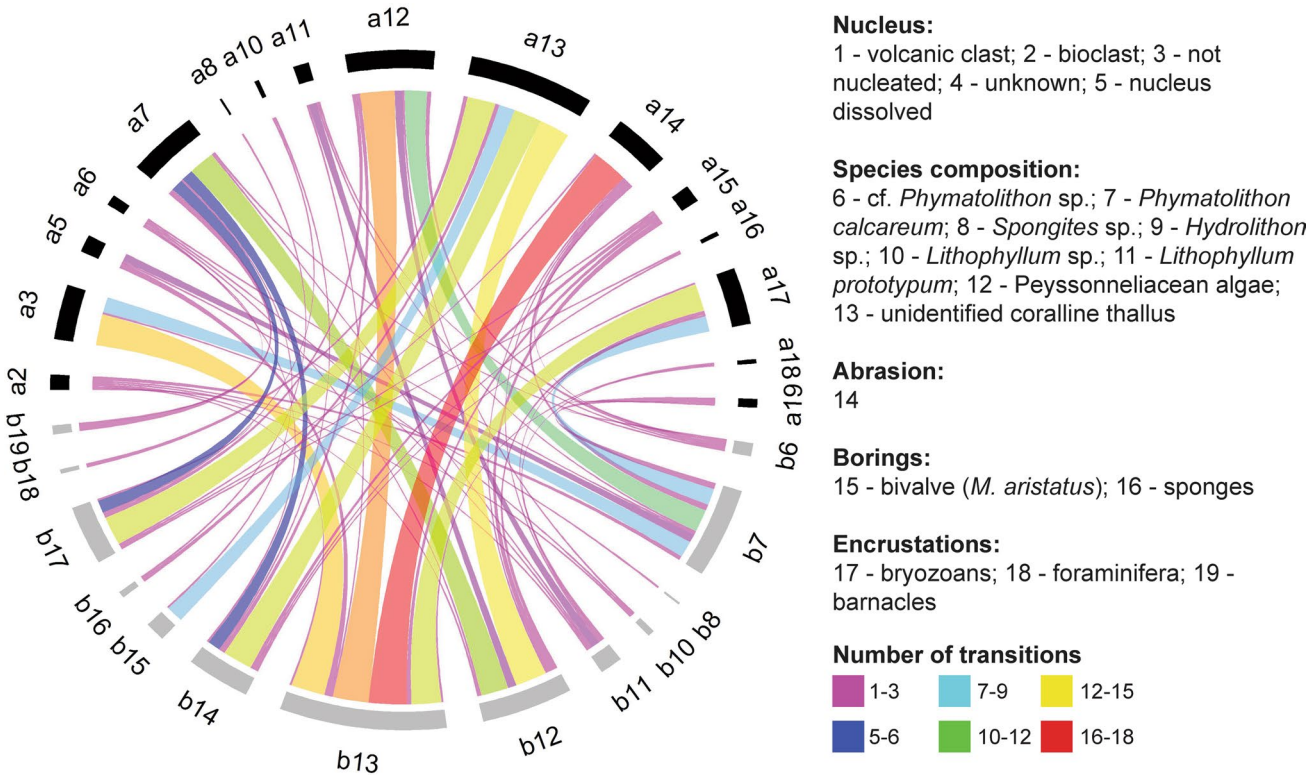

Fig. 8 Chord diagram representing the transitions in rhodolith composition (i.e., the successive organisms or structures composing the rhodolith—numbers from 1 to 18). The initial stages are represented in *black* and by the letter "*a*", the final stages are represented in *grey* and by the letter "*b*". As an example, a12 (peyssonnelliacean algae) and a14 (abrasion) are frequently followed by b13 (unidentified coralline thallus)

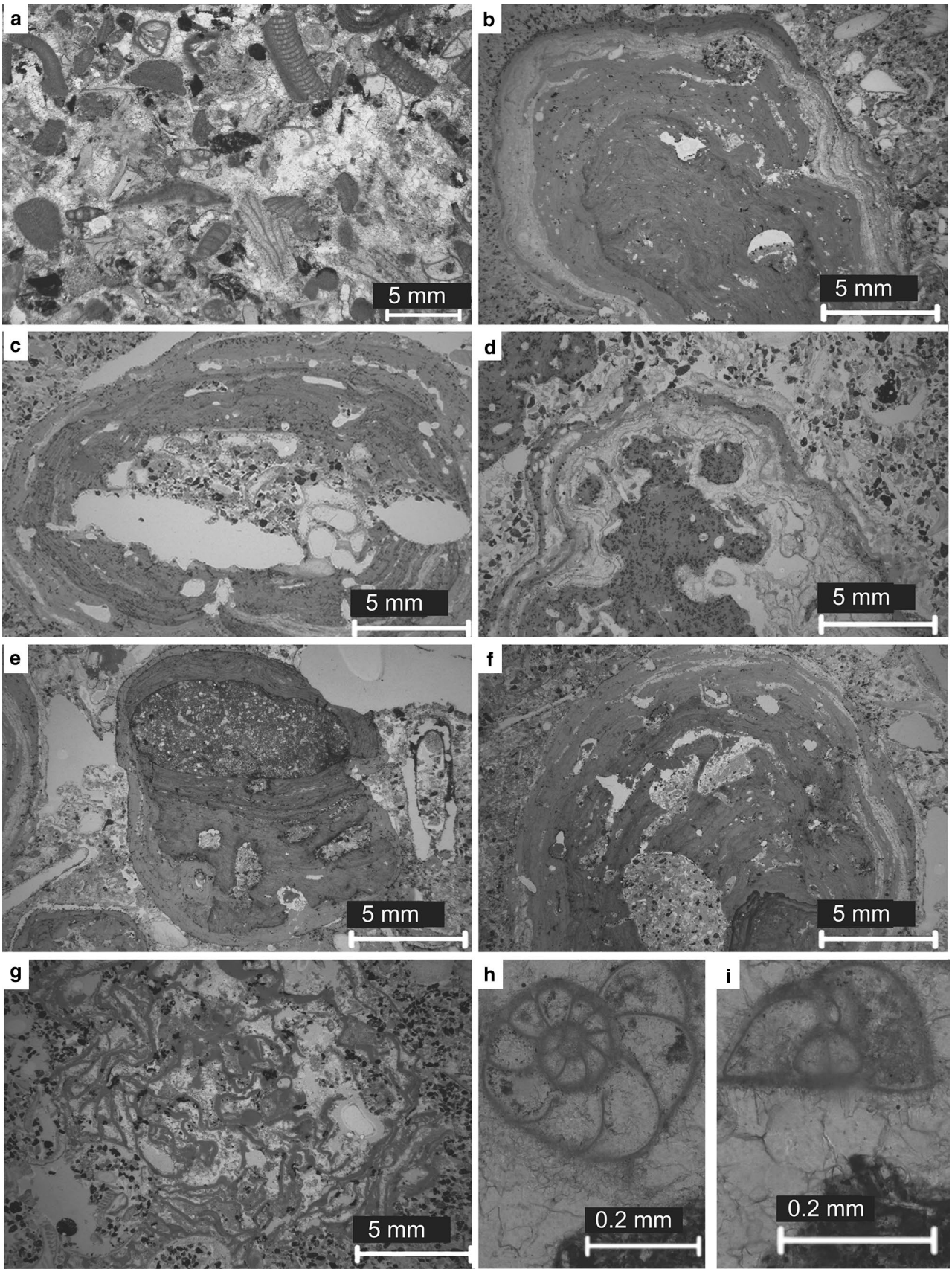
a
5 mm
b
5 mm
c
5 mm
d
5 mm
e
5 mm
f
5 mm
g
5 mm
h
0.2 mm
i
0.2 mm

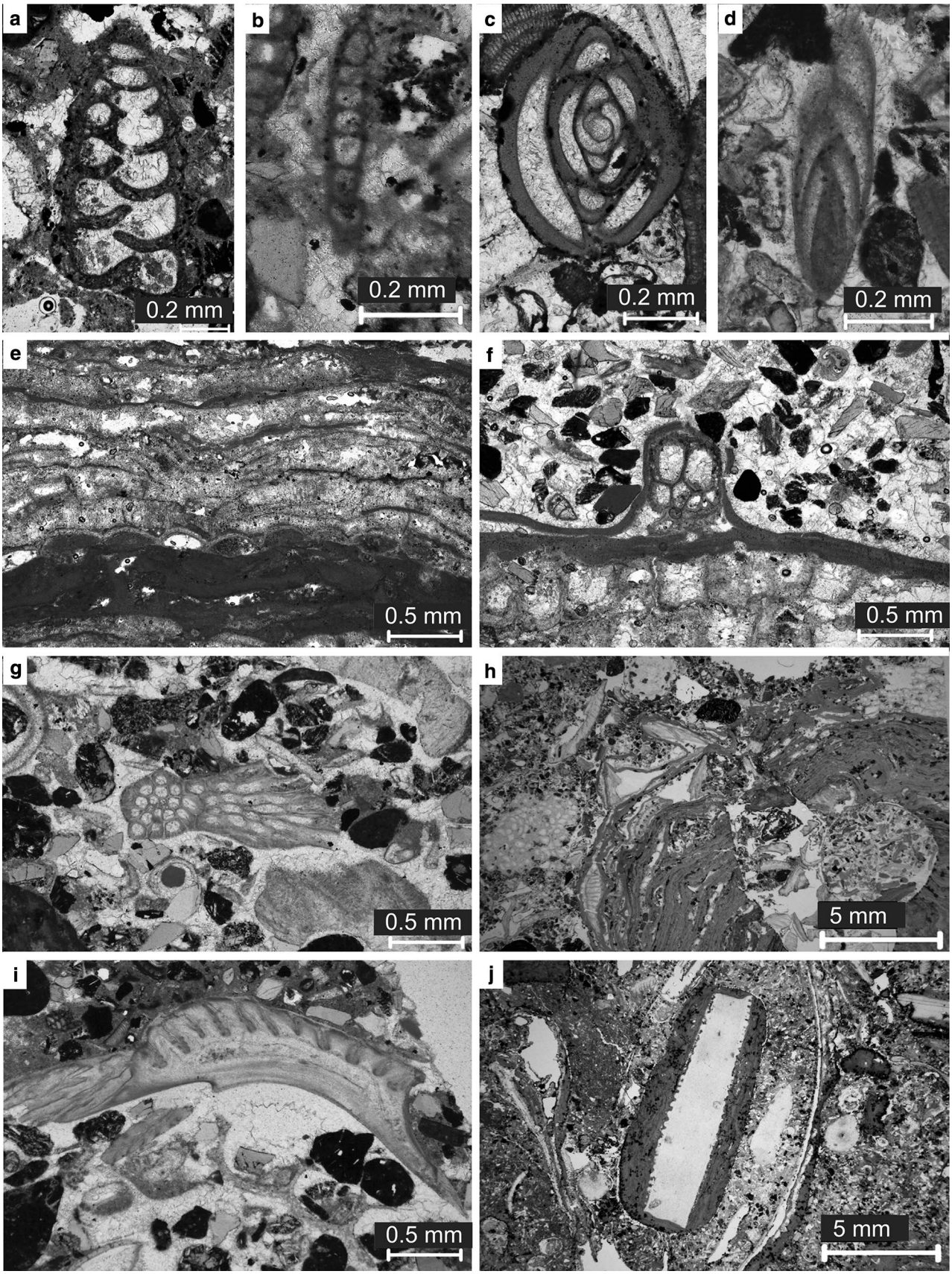
a
0.2 mm
b
0.2 mm
c
0.2 mm
d
0.2 mm
e
0.5 mm
f
0.5 mm
g
0.5 mm
h
5 mm
i
0.5 mm
j
5 mm

◀**Fig. 10** Thin-section components and details of encrustations. **a** Biserial textulariid foraminifer (thin-section: Malbusca B, facies 2b). **b** Uniserial textulariid foraminifer (thin-section: Malbusca B, facies 2b). **c–d** Miliolid foraminifers (thin-sections: Malbusca D, facies 2 and Malbusca C, facies 3 respectively). **e** Unilaminar bryozoan encrusting a coralline algae and being encrusted by peyssonneliacean algae (thin-section: Malbusca C, facies 2). **f** Coralline algae encrusting ?peyssonneliacean algae and a fragment of a (?semi)erect cyclostome bryozoan (thin-section: Malbusca C, facies 3). **g** Fragment of an erect bryozoan (thin-section: Malbusca A, facies 2b). **h** The barnacle *Z. santamariaensis* encrusting a rhodolith. The rhodolith is bored by two different organisms (thin-section: Malbusca D, facies 2). **i** Plate of the barnacle *Z. santamariaensis* (thin-section: Malbusca A, facies 2b). **j** Coralline algae growing around a cidaroid sea urchin spine (thin-section: Malbusca B, facies 2b)

within the upper triangle for spheroidal shapes, spreading into the sectors below to the right for ellipsoidal shapes.

Peyssonneliacean algae

In thin-section, the thallus of the peyssonneliacean alga *Polystrata alba* could be identified in most of the examined rhodoliths, alternating with the corallines. Isolated crusts and/or fragments were not recognized in the sediments (Fig. 9d).

Benthic foraminifera

In thin-section (Table 2) the hyaline foraminifera (Fig. 9h, i) are the most frequent taxa (12 %) followed by textulariids (8.3 %) (Fig. 10a, b), with miliolids accounting for the least frequent (5.3 %) (Fig. 10c, d).

Bryozoa

Bryozoans are represented by encrusting, nodular and erect growth forms. It is mainly encrusting unilaminar bryozoans that contribute to the rhodolith formation (Fig. 10e, f). Both fragments of encrusting (up to 8.3 %) and erect forms (up to 16 %) are present in the sediments in varying percentages (Fig. 10g; Table 2). The faunal composition of Malbusca is similar, albeit less diverse, to that reported from the Pedraque-pica outcrop about 4 km to the east (Ávila et al. 2015b). Some 13 cheilostome bryozoans could be determined to generic level (see "Appendix"), while several other cyclostome and cheilostome species were unidentifiable owing to poor preservation. Although most species produce encrusting unilaminar colonies, several taxa with erect colonies are also present (the bilaminar *Chaperiopsis*, the large robust *Metrarabdotos*, the fenestrate *Reteporella*, and several cyclostome species). One or more celleporiform species produce nodular colonies that encrust shells or occur free in the sediment.

Molluscs

The most abundant and diverse molluscs are the bivalves (see "Appendix"). These are represented by disarticulated valves of oysters, pectinids, the mussel *Myoforceps aristatus* and Noah's Ark shell *Arca noae*. In thin-section, fragments of both bivalves and gastropods constitute up to 3.2 % of the sediments (see Table 2).

Ostracods

Ostracods are restricted to the sandstone units and were studied by Meireles et al. (2012). They described 13 species, representing seven families and 12 genera (see "Appendix").

Barnacles

Malbusca is the type locality of the barnacle *Zullobalanus santamariaensis* (Winkelmann et al. 2010). It occurs on the outer surface of rhodoliths (Fig. 10h) in facies 3 and as debris in the units above, where it represents up to 8.3 % of the bioclasts (Fig. 10i). Only in one case it directly encrusts the basaltic basement (log F, Fig. 7a).

Echinodermata

Echinoderms occur throughout the exposure, mostly as fragments and loose spines, more rarely as whole specimens. Madeira et al. (2011) identified six species (see "Appendix"). In thin-section, their spine fragments constitute up to 6.1 % of the sediments and the test fragments up to 7.2 % (see Table 1). Some echinoid fragments served as nucleus for rhodoliths (Fig. 10j).

Calcareous nannofossil assemblages

Samples of calcareous nannofossils were collected from the sandstone layers at 3 levels in section Malbusca B and at 5 levels in section Malbusca D (see Fig. 2). In both sections, assemblages can be characterized by relatively low abundance and diversity, consistent with the shallow-marine paleoenvironment. Both total abundance and diversity show a general trend to decrease up-section.

The identified taxa are listed in the "Appendix". The co-occurrence of *R. rotaria* and *R. pseudoumbilicus* suggests a late Miocene (Messinian) age (6.9 and 5.9 Ma, Nannotax 3 ranges). While the occurrence of *R. pseudoumbilicus* is well established, *R. rotaria*, is rarer in the assemblage and more problematic to confirm. In the absence of further stratigraphic markers, the biostratigraphic age should be treated with caution.

Discussion and interpretation

Paleoenvironmental indicators

Geological background

The volcano-sedimentary sequence at Malbusca corresponds to the subhorizontal stacking of thick submarine lava flows and subordinate intercalated marine sediments, up to ~130 m a.s.l. (above present sea level), where the transition to subaerial volcanic products crops out (see Fig. 1). The overwhelming majority of the submarine volcanic products correspond to tabular sequences of pillow lavas (with no interstitial hyaloclastites) and laterally extensive subhorizontal or gently dipping submarine sheet flows of metric to decametric thicknesses. These products imply the subaqueous emplacement of lava flows under high to very high extrusion rates, over a flat or gently dipping bottom, with a gradual filling of accommodation space mostly by aggradation and to a lesser extent by progradation (see Fig. 4b of Ramalho et al. 2013). At some point the transition to a subaerial environment occurred, showing that all the available accommodation space was locally filled and marine deposition ceased.

As established in "Stratigraphic logs", the basal set of submarine lava flows (where the main sedimentary sequence sits) is truncated by an unconformity eroded through wave action. This implies a small relative sea-level drop between the extrusion of the lava flows (in subaqueous conditions) and the formation of the erosive surface by surf action. However, above this unconformity, the volcano-sedimentary deposits that stacked up to form the sequence are entirely submarine up to ~130 m a.s.l. The succession therefore denotes a rapid relative sea-level rise between the erosive unconformity and the transition to subaerial products at ~130 m a.s.l.; this relative sea-level rise occurred, approximately, between 4.32 ± 0.06 and 4.02 ± 0.06 Ma, as suggested by the geochronology of Sibrant et al. (2015).

Paleoecological proxies

Coralline algae

The most important limiting factor for the distribution of coralline algae seems to be light intensity, correlated with depth and geographical latitude (Bourrouilh-Le Jan and Hottinger 1988; Rasser 1994 and references therein). For instance, Wisshak et al. (2010, 2015) recently showed that in the Azores coralline red algae thrive on both the upper and lower surfaces of settlement panels deployed down to 15 m whereas they occur only on the upper surfaces of panels deployed at 60 m, and are entirely absent from the deeper stations. The fragments of geniculate coralline algae are most typical for intertidal to very shallow subtidal, high-energy environments (Cabioch et al. 1992).

Rhodoliths

Composition and encrustation sequences Taxonomic successions within a rhodolith may be the result of transportation and/or environmental change.

In this study, the primary rhodolith builder is *Phymatolithon calcareum*, which has been recorded from the Mediterranean and Pannonian basins since the Oligocene (Braga et al. 2009), and is also reported for the Pliocene of Spain (Braga and Aguirre 2001). This species, due to its wide thermal tolerance, is both very common and widely distributed. It can be found from intertidal and subtidal grounds (down to 32 m depth) all across the Atlantic from the Arctic to the Antarctic, the Mediterranean Sea, the Caribbean region, the Red Sea and the Pacific Ocean (Rosas-Alquicira et al. 2009; Guiry and Guiry 2015). Today, *P. calcareum* is known from the Azores as a rhodolith-forming species in a protected shallow (2–4 m depth) bay at Lajes do Pico, Pico Island (Rosas-Alquicira et al. 2009; Rebelo et al. 2014). According to Aguirre et al. (2012) *P. calcareum* is one of the major components of the rhodolith-rich lithofacies in the southern Balearic platform at 35–100 m depth, in the central Tyrrhenian Sea at 25–100 m (greatest abundance at 60–70 m), and in the Gulf of Naples at 35–40 m. The formation of thick rhodolith beds has been proposed as an indication for transgressive deposits and/or storm-deposits (Johnson et al. 2011, 2016).

Lund et al. (2000) reported that peyssonneliaceans are also recorded as abundant components of the calcareous algal flora in depths greater than several tens of meters; and that melobesioid-dominated assemblages within fossil nodules have been used as an indication of growth in deep waters ranging from the Cenozoic off northeastern Australia and the Eocene of northern Italy.

According to Basso et al. (2009) the corallines forming rhodoliths die when washed ashore by storm waves, or when buried by sediment for a considerable time span (i.e., several months). In the intertidal zone, the rhodoliths can be abraded in the swash zone, bored, or immobilized in crevices; if a dead rhodolith re-enters the shallow subtidal zone, it can be further bored or, alternatively, a new coralline thallus can cover the older abraded and bioeroded rhodolith. The cycle can be repeated until the rhodolith reaches a critical size, beyond which it cannot be moved anymore and other encrusting organisms are likely to grow over it in time. Thus, frequency of disturbance, depth of origin, and possibly nutrient supply determine the diversity and degree of other photoautotrophic and heterotrophic organisms contributing to rhodolith formation (e.g., Lee et al. 1997).

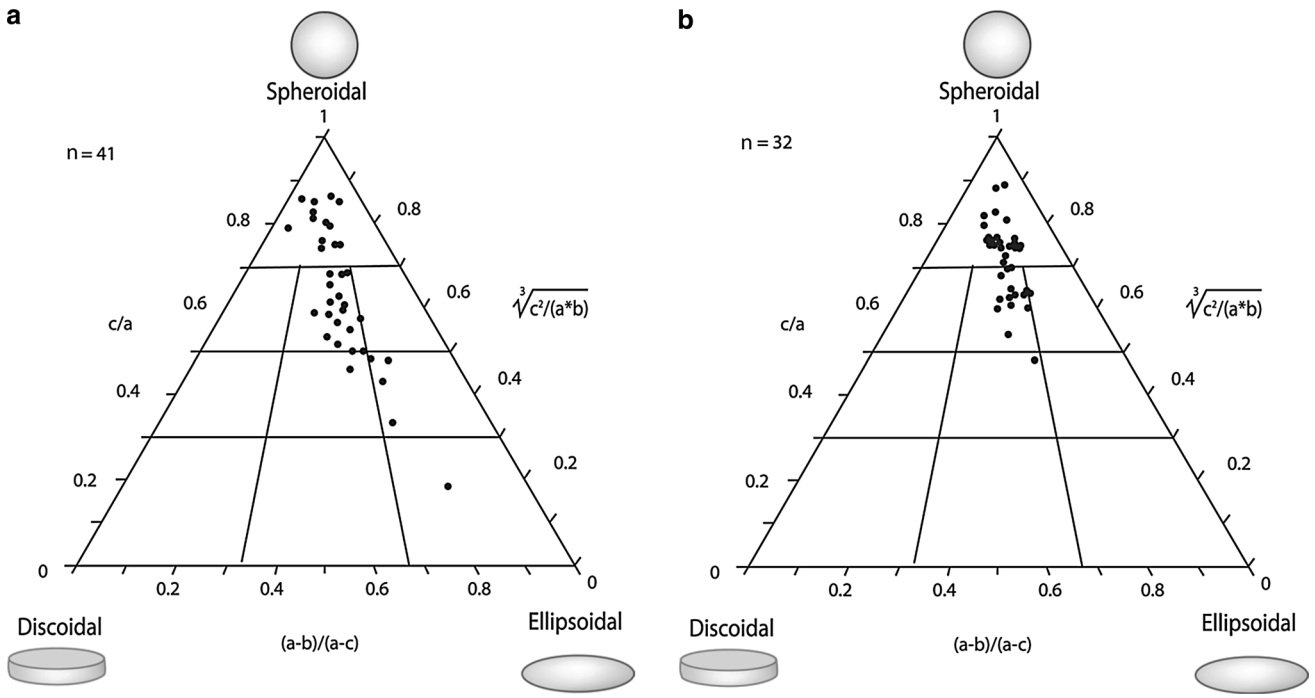

Fig. 11 Triangular plots showing the relative shapes of fossil rhodoliths: **a** from the center of the basal unit with rhodoliths at Malbusca B and **b** from the center of the basal unit with rhodoliths at Malbusca D. Shape classification according to Sneed and Folk (1958)

Among the rhodoliths from Malbusca, encrusting bryozoans are consistently overgrown by either corallines or peyssonneliaceans, suggesting a temporal disturbance in the rhodoliths growth that allowed the bryozoans to grow for a short time before the red algae prevailed again. Barnacles, on the other hand, tend to occupy the outer surface of the rhodoliths, being only occasionally overgrown by corallines. This shows that barnacle encrustation took place during the final stage of rhodolith growth, or after death of the rhodolith-forming corallines.

Size and shape The final shape of a rhodolith is considered to be the result of species-specific growth habit and degree of water motion (Steller and Foster 1995; Basso et al. 2009). The majority of the very shallow water rhodoliths reported in the literature are spheroidal to ellipsoidal in shape, with a fruticose growth form (Basso et al. 2009).

The shapes of the rhodoliths from Malbusca are independent of the shapes of their nuclei, which is mainly due to their thickness and expected higher age. The classical shape classification diagram of Sneed and Folk (1958) in Fig. 11 suggests high-energy conditions during the rhodolith growth history with multidirectional transport directions.

Bioerosion, abrasion, and fracturing All rhodoliths studied herein show abrasion and fragmentation. Such destructive processes that remove or degrade rhodoliths have been linked to the effects of either physical disturbance or biological erosion (Basso and Tomaselli 1994; Checconi et al. 2010). Boring preservation reflects both the intensity of abrasion and the rhodolith overturning frequency. The frequent occurrence of borings truncated by abrasion at different depths within the rhodoliths along with the presence of younger borings cutting older ones indicates the succession of several destructive events during rhodolith growth (Checconi et al. 2010) thus attesting for "rocking" around the volcanic island shelf.

The intense bioerosion with the contribution of bivalves is typical for the *Entobia* ichnofacies, which requires several months or years of exposition before burial (Bromley and Asgaard 1993; de Gibert et al. 1998).

Life history of rhodoliths The environmental factors responsible for the genesis of thick, dense concentrations of rhodoliths over long timespans are not well known. Rhodolith beds can be preferentially associated with transgressive deposits, but the ecological conditions required to produce profuse rhodolith growth can also be achieved in other contexts of sea-level variation (Aguirre et al. 2012).

The implication for the studied rhodoliths is that they were repeatedly abraded and fragmented due to hydrodynamic energy. After fragmentation/abrasion, a certain time of quiescence and stability occurred that allowed boring by bivalves and sipunculids. Afterwards, the environmental conditions again became suitable for encrustation by

corallines. The repeated occurrence of all of these features suggests a highly dynamic system. At the very end of their life history, many rhodoliths were encrusted by barnacles, which suggest a shallow-water final stage with high substrate stability suitable for barnacle growth.

Fossil rhodoliths from other Atlantic Archipelagos and elsewhere Comparison of size, morphology, shape, and species composition of the rhodoliths from Malbusca with others from the Macaronesian archipelagos (Madeira, Canary Islands and Cape Verde) reveals that the fossil rhodolith accumulations in these islands all correspond to storm deposits, although they show considerable differences.

Shape analysis of rhodoliths, both fossil and modern, is a useful way to supplement the criteria for assigning rhodolith deposits to a given depositional model. The format using triangular plots for rhodolith shapes (Bosence 1976, 1983) draws distinctions among spherical, ellipsoidal, and discoidal shapes. The shape of Cabeço das Laranjas rhodoliths from Ilhéu de Cima on Porto Santo in the Madeira Archipelago (Johnson et al. 2011, their Fig. 7) includes a range of perfectly spherical specimens as well as those that are slightly more ellipsoidal in shape. This spread in shapes overlaps to some extent with those from Malbusca (Fig. 11), whereas those from Porto Santo are much larger in size and come from a deposit more than twice as thick as the maximum Malbusca deposit. A better fit with the Malbusca rhodoliths in size and shape is shown by a sample of Pleistocene rhodoliths from the locality Portinho da Mulher Branca on Santiago in the Cape Verdes (Johnson et al. 2012, their Fig. 9f). Those are regarded as having been deposited as a result of shoreward transport against a basaltic coast with an undulating topographic surface having a maximum relief of 4 m. This scenario is reminiscent of the uneven paleotopography at Malbusca, although the spatial separation of basalt highs on the southeast Santiago coast is on the order of 75–100 m; whereas the basalt highs at Malbusca are much more closely spaced.

Modern rhodoliths occurring on the north shore of Fuerteventura in the Canary Archipelago (Johnson et al. 2012, their Fig. 9f) also match the shapes of the Malbusca rhodoliths, although the Fuerteventura rhodoliths are smaller in diameter. The Fuerteventura sample represents an overwash deposit more than a meter in thickness that crossed a wide rock platform eroded in basalt. The source of this deposit is from a living rhodolith bank in water up to 30 m deep located 2–3 km offshore. Another reasonably good match with the size and shape of Malbusca rhodoliths comes from a fossil deposit comparable in age from the northern, windward shores of São Nicolau in the Cape Verdes (Johnson et al. 2014, their Fig. 5a–c). Ellipsoidal-shaped rhodoliths are less common in the São Nicolau deposits than in the Malbusca deposits. Another critical difference is that the São Nicolau rhodoliths are mostly nucleated around basalt pebbles, whereas the Malbusca rhodoliths rarely have basalt nuclei. The Miocene São Nicolau rhodoliths are interpreted as having been transported shoreward from a nearby rhodolith bank. The rhodoliths came to rest in deposits up to 2 m thick against a basalt shore without variations in topographic relief, but with overhanging ledges under which rhodoliths were impressed.

At the opposite extreme, it is possible to contrast the Malbusca rhodolith deposits with markedly different ones, such as Miocene rhodolith deposits from Ilhéu de Baixo in Porto Santo in the Madeira Archipelago that are interpreted as submarine slump deposits on an active volcanic slope (Baarli et al. 2014). In this case, very few whole rhodoliths occur in a matrix dominated by crushed rhodolith debris. One of the few fossil rhodolith deposits regarded as having been preserved in life position comes from the west side of Ilhéu de Cima in Porto Santo, where a sample of spherical to somewhat ellipsoidal rhodoliths is encrusted around very large pebbles or small cobbles, immediately adjacent to basaltic knobs with a topographic relief of about 1 m. The rhodoliths occur in a thin deposit scattered among the protruding basalt knobs, their cover rarely exceeding two vertical layers of rhodoliths (Santos et al. 2012). The distribution of shapes is very similar to the Malbusca rhodoliths, but the Ilhéu de Cima rhodoliths are much larger in diameter and all are nucleated around large basalt clasts. The large clast size is directly attributed to a proximal source in the eroded basalt knobs.

It may be argued that rhodoliths with a propensity towards shapes that are highly spherical may grow in places where the water depth is sufficiently shallow to promote frequent motion in rough water. Where fossil rhodoliths are nucleated around pebbles and small cobbles, it may be argued that they originated in relatively shallow water, close to a rocky shoreline (Santos et al. 2012; Johnson et al. 2014).

Thus, among the various published studies that examine living and fossil rhodoliths from volcanic islands of the northeastern Atlantic Ocean, those from the Pleistocene of Santigo at Portinho da Mulher Branca and from the Miocene on the northeast side of São Nicolau, as well as the modern rhodoliths from the north shore of Fuerteventura most closely resemble the size and shape of the Malbusca rhodoliths. There are significant differences in geographic setting, but the three examples in this comparison all share an interpretation of shoreward transport away from an original source in living banks. The variation in topographic relief produced by the basalt substrate on which the Malbusca rhodoliths sit is substantially smaller and more closely spaced than found on the southeast shores of Santiago in the Cape Verde Archipelago. The erosional features

exposed at Malbusca were most likely formed as surge channels that became increasingly shallow in the landward direction. It appears that rhodoliths in the basal deposits from this locality were trapped and accumulated first in the lowest parts of the depressions, but eventually filled toward the tops and even overlapped against the sides of the basalt highs.

Ichnology

The presence of ichnofossils in the sandstone units is believed to represent colonization of the substrate following a storm in a time of quiescence. The sandstone units in the Malbusca logs A–C are intensively bioturbated with *M. segregatis*, which in several horizons are preferentially oriented vertically (Uchman et al. 2015). Thicker layers with abundant *M. segregatis* are typical of foreshore sediments (e.g., Pemberton et al. 2001, 2012; Seike 2007) and the vertical orientation in the section studied is referred to tides influencing migration of the mixing zone between the marine and fresh waters (Uchman et al. 2015, 2016). *Psilonichnus* is a typically upper foreshore-backshore trace fossil (*Psilonichnus* ichnofacies; see Buatois and Mángano 2011) but its occurrence (only at Malbusca log A) is not sure. *Ophiomorpha nodosa* (probably *Ophiomorpha* isp. belongs to this ichnospecies) is most common in the lower foreshore-upper shoreface in the *Skolithos* ichnofacies (Pemberton et al. 2001). *Piscichnus* is an intertidal and shallow subtidal form (Gregory 1991). However, the presence of confined horizons with the generally horizontal *Bichordites* or *Thalassinoides* indicates a more quiet environment, more suitable for the *Cruziana* ichnofacies. The association of horizontal and vertical (especially *Ophiomorpha*) trace fossils allow an assignment to the proximal *Cruziana* ichnofacies, which is typical of the shoreface, foremost of the upper shoreface conditions (cf. Pemberton et al. 2001). A bed with *Bichordites* just above rhodoliths in the Malbusca log D points to deeper conditions. The *Macaronichnus–Ophiomorpha–Piscichnus* that follow above are an evidence of a more energetic, probably shallower environment. The less energetic conditions repeat again as marked by the next horizon with *Bichordites*. The thick bed of sandstone (Malbusca log D, facies 5b) shows colonization by burrowing ichnofauna only from the top (represented by *Ophiomorpha* and *Macaronichnus*) indicating a shallow subtidal environment. The overlying beds of sandy calcarenite (facies 6) are characterized by trace fossils of intertidal and shallow subtidal environments (*Ophiomorpha* isp., mostly horizontal *M. segregatis*, *Piscichnus* isp.), which occur with trace fossils typical of the slightly deeper *Cruziana* ichnofacies (*Bichordites*, *Dactyloidites ottoi*). This, together with the storm origin of the beds, suggests the proximal *Cruziana* ichnofacies indicating an upper-middle shoreface setting. *Dactyloidites ottoi* is considered as typical of nearshore to deltaic, siliciclastic settings rich in food, within the "lower *Skolithos* and upper *Cruziana* ichnofacies" (Wilmsen and Niebuhr 2013). Tracemakers of the trace fossils belong to deposit-feeding opheliid polychaetes (*Macaronichnus*), onuphid or oweniid polychaetes (*Diopatrichnus*), unknown polychaetes, maybe carnivorous (?*Palaeophycus*) and deposit feeding "worms" (*Dactyloidites*), omnivorous crabs (?*Psilonichnus*) and decapod crustaceans (*Ophiomorpha*, *Thalassinoides*), deposit-feeding irregular echinoids (*Bichordites*), and carnivorous ray fishes (*Piscichnus*). These animals need oxygenated waters, which can be pumped into the open burrows of crustaceans and polychaetes. The opheliid polychaetes producing *Macaronichnus* obtain oxygen from pore waters. The irregular echinoids producing *Bichordites* can burrow close to the redox boundary several centimeters below the sediment surface (Bromley et al. 1997).

Invertebrates

Molluscs are the most abundant group of invertebrates at Malbusca and the specific composition of the paleocommunity suggests an agitated, shallow subtidal environment. Nearly all bivalve shells are disarticulated and 90.4 % have broken edges ($n = 374$ valves) (log A, facies 2b and log C facies 2), suggesting a strong hydrodynamical depositional setting. However, fragile elements of the sculpture of the shell (e.g., spines) are still preserved in many specimens examined. Shells are deposited with no preferential settling position and this chaotic disposition is typical of storm deposits. Comparison with modern relatives indicate presence of hard substrates interspersed with soft bottoms at Malbusca.

Barnacles are abundant in the matrix indicating the presence of suitable hard substrates. The abundant barnacles encrusting the rhodoliths demonstrate also that the latter provided sufficient substrate for barnacle growths. The same is true for the presence of geniculate corallines. They could have derived from a rocky shore surrounding the rhodolith depocenter but may also have lived on the rhodoliths in a very late stage of rhodolith formation.

The rhodoliths are only rarely encrusted by unilaminar bryozoans that, therefore contribute little to the rhodolith/macroid mass. It is likely that disturbance of the rhodoliths occurred too frequently for bryozoans to thrive as other growth forms are also rarely found in the rhodolith beds. Bryozoans become more diverse and abundant in the shell rudstone, in which encrusting growth forms prevail,

Table 3 Calcareous nannofossil total abundance and diversity

Section/Stratigraphic units	Coccolith abundance index				Small %				Paleobiodiversity			
	Min	Median	Max	Std	Min	Median	Max	Std	Min	Median	Max	Std
Malbusca log B												
Upper sequence												
Upper part	30	49	80	25.2	83	86	86	1.7	4	6	7	1.5
Lower part	1	53	70	35.9	0	67	68	39	1	6	8	3.6
Lower sequence												
Upper part	40	141	191	76.9	60	69	77	8.5	7	7	10	1.7
Malbusca log D												
Upper sequence												
Upper part	2	9	11	4.7	0	64	78	41.6	2	3	4	1
Middle part	22	36	133	60.5	73	75	80	3.6	5	6	11	3.2
Lower part	11	34	96	44	73	76	78	2.5	5	5	8	1.7
Lower sequence												
Upper part	4	7	11	3.5	33	45	100	35.7	2	5	6	2.1
Lower part	6	34	67	30.5	17	65	73	30.3	4	5	8	2.1

covering bivalve shells and occurring free as multilaminar bryozoan macroids. Although erect, rigid, branching bryozoan growth forms are usually associated with deeper waters, especially in high-energy conditions such as in offshore islands, it may also be likely that the erect *Metrarabdotos*, *Reteporella* and several cyclostomes found in Malbusca lived in cryptic habitats. In the Azores these colony types are today found in protected cracks, crevices and caves as well as underneath rock overhangs as shallow as 10 m (BB pers. observ.).

The echinoderm community of Malbusca is dominated by remains of the cidaroid echinoid *Eucidaris* in the rhodolith bed, which typically inhabits shallow-water habitats in the Caribbean today (often associated to coral reefs and other firm-ground habitats). Upsection, irregular echinoids of the genera *Echinocyamus* and *Clypeaster* become more common, suggesting a change of the source area of the tempestites, since these taxa typically inhabit shallow sand bottoms or seagrass meadows (Madeira et al. 2011).

Ostracods are mainly benthic epifaunal detritivore-grazer species. Within the ostracod assemblages at Malbusca, only one species out of the 13 Mio-Pliocene taxa reported for this outcrop still occurs nowadays in the Azores (*Loxoconcha rhomboidea*) in shallow-water environments (from the intertidal zone down to 40 m depth) (Meireles et al. 2012, 2014).

Calcareous nannofossil assemblages are poorly diverse and dominated by placoliths with a reduced presence of asteroliths and sphenoliths which supports sedimentation in a shallow-marine paleoenvironment. A certain degree of variability (see Table 3) among replicates of the triplet sets of samples also argues in favor of high coastal hydrodynamic conditions. Surprisingly, the triplets collected from the coarser base of the sequences tend to have a slightly higher abundance and diversity of calcareous nannofossils than the uppermost sectors. At first these results indicate no clear transgressive or deepening trend along the (B and D) sequences. A possible explanation may result from an initial period of sediment starvation associated to a rapid local sea-level rise and inland migration of the coast-line that led to richer calcareous nannofossil assemblages at the base of the sequences. After a certain period of time progradation of the coastal sedimentation reached the Malbusca sections, leading to the dilution of the calcareous nannofossils as found towards the top of the sections.

There is also a possibility that coastal hydrodynamics during storm events might have reworked late Miocene forms, which could also explain the incongruent nannofossil biostratigraphic dating.

Sedimentological considerations

The studied succession reveals a general fining-upward trend in agreement with Meireles et al. (2012), who suggested that the progressive reduction in grain size of the constituents of all studied samples, collected from the bottom to the top of the sequence, indicates a decrease in hydrodynamic energy during the sedimentation process.

The succession is, however, interrupted by several erosional truncations providing clear evidence for the multiphase nature of deposition. The trace fossils on top of the units suggest times of quiescence after the hydrodynamic events that stimulated sediment transport. Also the horizons with *Bichordites* isp. point to a less energetic (deeper) environment than in the surrounding sediments with *Macaronichnus*, *Ophiomorpha* and *Piscichnus*, which indicate more energetic (shallower) environments. Such less energetic horizons may be related to flooding pulses during the general transgression, resulting in the increasing accommodation space. The space is filled by sediments leading to a shallowing indicated by a recurrence of the *Macaronichnus–Ophiomorpha–Piscichnus* ichnoassemblage. Direct evidence of storm activity and sediment redeposition (Tucker 2003; Johnson et al. 2011) comes from the hummocky cross-stratification retained in the sandstone unit (e.g., log D, facies 5c).

As this implies transport of the sediments, the question arises as to where the original environment of the bioclasts, i.e., the carbonate factory (Schlager 2003), may have been situated: further on shore or offshore? In either case, the site is not exposed today as it is either covered by volcanic rocks or positioned below the sea-level, respectively. The abundance of carbonate particles in the sediment and the low frequency of basaltic rhodolith nuclei suggest an environment with low influx from the surrounding basaltic substrate. This is in agreement with the inference that the island edifice, was at the time, a wide and shallow submarine bank with possibly only a few residual reliefs or penecontemporaneous surtseyan cones above sea level (Ávila et al. 2012; Meireles et al. 2013); carbonate productivity was enhanced by a combination of a favorable and variable topography (creating a shallow, flat bottom with sandy and rocky substrata) and warmer waters (Ávila et al. 2016).

Autochthony versus transport

Another crucial paleoenvironmental question is whether or not the rhodoliths were formed/living at the place where they were deposited at the end, i.e., within up to 2-m-deep pools between the eroded pillow lavas. The evidence of platy coralline red algae encrusted around large autochthonous cobbles within the pools and barnacles encrusting the tops of basalt knobs show that such shallow-water pools existed indeed.

Three possible scenarios that bear comparison entail models for: (1) the onshore transport of rhodoliths as a result of coastal over-wash due to storm surge; (2) fragmentation and diffusion of rhodoliths at a water depth close to storm wave-base; and (3) significant offshore, down-slope transport due to counter-surge of storm water or perhaps mass gravity flows due to instability of shelf deposits.

Johnson et al. (2012, their Fig. 12) developed an overall scheme for the marine transport of rhodoliths with an emphasis of nine potential scenarios characteristic of regional variation. In a search for a model that best fits the Malbusca locality, it is not difficult to eliminate several that are clearly inappropriate. For example, the basal rhodolith deposits at Malbusca clearly are not typical of beach, berm, or dune deposits. Nor are they representative of tsunami deposits or hurricane deposits.

Where rhodoliths are autochthonous nowadays, they live in a shallow environment similar to that found at Lajes do Pico (Pico Island, Azores) as described by Rosas-Alquicira et al. (2009) and the vast majority has a basaltic nuclei. In our opinion, those rhodoliths predominantly lacking rock cores (which are the most abundant at Malbusca) lived further offshore and were transported onshore from deeper environments.

Depositional model

From the above discussion and the comparison with other rhodolith deposits, we suggest that some of the Malbusca rhodoliths were living in the basaltic depressions where they are found today, because autochthonous crusts on the basalt occur. However there are signs of transport because rhodoliths are abraded and are part of a tempestite sequence. The multiphase events that led to the formation of the sedimentary sequence at Malbusca can be roughly summarized as shown in Fig. 12. Initially to the south of today's cliff-line at Malbusca, most of the observed biota lived on a shallow rocky shelf where large bivalves as well as *E. tribuloides* sea-urchins thrived. Pockets of bioclastic sands included a few, mostly nucleated, rhodoliths. At slightly greater depths, soft bottoms were the dominant setting, with a large population of mainly non-nucleated rhodoliths and other soft-sediment associated species (e.g., the echinoids *C. altus* and *E. pusillus*) (Fig. 12a). As today, the shores of the island were subject to episodic storm events, as expressed by the repeatedly broken rhodoliths. Hence, stronger storm events led to the formation of proximal tempestites (e.g., tempestites with a position close to shore) that remobilized and transported huge amounts of sediment onshore. As it is typical for tempestites, the heaviest particles, i.e., the rhodoliths, were deposited first, and higher up in the section, bivalve shells, hummocks, laminated sediment, and trace fossils follow at the top marking the transition to fair-weather conditions (Fig. 12b). It follows that subsequent events triggered the formation of additional

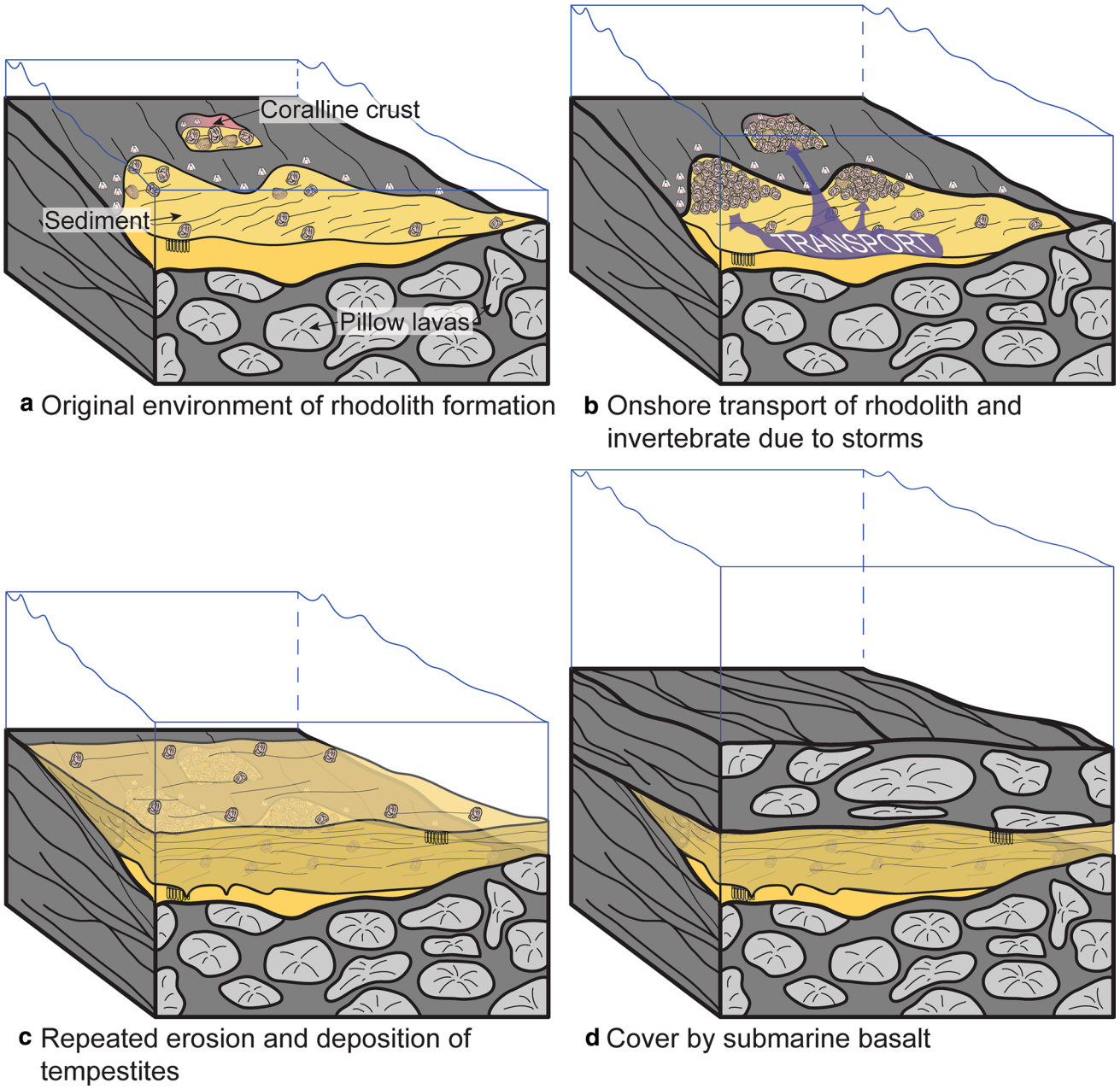

Fig. 12 Schematic reconstruction of the Pliocene sedimentary sequence of Malbusca. For details see text

tempestites that erosively cut into the older tempestite and formed channels that were additionally filled by fining-upward sequences (Fig. 12c). Finally, the whole sedimentary sequence was covered by submarine lava flows that contributed to its preservation, being nowadays exposed by means of uplift and erosion of the coastline (Fig. 12d).

The aforementioned succession of events therefore resulted in an amalgamation of sedimentary packages, which exhibit a general fining-upwards trend, as well as internal normal grading. The gradual—but stepped—transition between coarser clast- to matrix-supported sediments to thicker but finer calcarenites with hummocky and swaley cross-stratification denotes a decrease in energy during the sedimentation processes, i.e., increasing water depth. These characteristics are typical of many oceanic island marine sequences (e.g., Ramalho 2011; Ramalho et al. 2013; Meireles et al. 2013; Mayoral et al. 2013; Johnson et al. 2014; Ávila et al. 2015a, b), which denote rapidly rising relative sea levels before burial by volcanic activity. A general transgressive trend, in the case of Malbusca, is also attested by the characteristics of the overall volcano-sedimentary sequence, which feature a stacking

of submarine volcanic products and marine sediments to ca. 130 m above present sea-level, where the transition to subaerial products crops out today. Since this transition is presently ca. 110 m above the described rhodolith beds, a rapid sea-level rise must have occurred within the period comprehended between rhodolith deposition and the transition to a subaerial environment. According to the sea-level curve of Miller et al. (2005) and using the 4.32 ± 0.06 and 4.02 ± 0.06 Ma age interval provided by Sibrant et al. (2015) for the Malbusca sediments, at about 4.255 Ma there is a sea-level fall to −34 m, followed by a sea level rise to +3.2 m at 4.245 Ma. This 10 ka time-interval could correspond with the period of inferred relative sea-level rise, which would be penecontemporaneous with the deposition of the rhodoliths and sediments above the rhodolith beds. Between 4.015 and 3.995 Ma, a relative sea-level fall of 59.6 m occurred (from +3.2 to −56.4 m) and from 3.995 to 3.86 Ma, a relative sea-level rise trend occurred, reaching a maximum elevation of +22.1 m at 3.86 Ma, the corresponding total sea-level variation amounting at 78.5 m. According to Ramalho et al. (2014), during this whole time interval (i.e., 4.255–3.86 Ma) the island was subsiding at an estimated rate of ~100 m/Ma, which thus corresponds to a total subsidence of about 39.5 m. Therefore, adding the subsidence trend to the relative sea-level rise gives a total of 118 m, thus explaining the relative sea-level rise of 110 m deduced from the volcano-sedimentary sequence.

Conclusions

The study of the rhodolith accumulations from the Malbusca section of Santa Maria Island together with their sedimentary microfacies allow the following conclusions:

1. The rhodoliths are multispecific, mostly non-nucleated, with rare shells or volcaniclasts as nuclei.
2. Rhodoliths measure between 2 and 8 cm in diameter and their size and shape are independent of the size and shape of the nuclei. The majority of rhodoliths show a laminar-concentric growth form. The shapes are spheroidal with a slight tendency to ellipsoidal forms suggesting high-energy conditions during their growth history with multidirectional transport directions. The rhodoliths consist of a complex succession of encrusting coralline algae, peyssonneliacean algae, subordinated bryozoans and barnacles. Barnacles usually occupy the outer side of the rhodolith, being only occasionally overgrown by the corallines, suggesting that encrustation took place after final deposition of the rhodoliths, which then remained in a more or less stable position. It also suggests that the rhodoliths were transported to a shallow-water final resting place, where they were colonized and encrusted by *Zullobalanus*. The bioerosion, abrasion and fracturing present in all rhodoliths are associated with the effects of storms.
3. Other biogenic components present in the rhodolith rudstone include fragments of geniculate coralline algae, benthic foraminifera, bryozoans, molluscs, barnacles and echinoderms. The fauna present in Malbusca is a mixture of benthos living on hard and soft substrates in an agitated, shallow subtidal environment.
4. The beds above the rhodolith rudstone include, among others, tempestite layers, thin shell-beds and hummocky cross-stratification, and end in heavily bioturbated sandstones that are capped by penecontemporaneous basaltic submarine sheet flows.
5. The Malbusca sequence was formed by multiphase storm events that resulted in an amalgamation of sedimentary packages, which exhibit a general fining-upwards trend, as well as normal grading. This is typical for a transgressive sequence. A general transgressive trend is also attested by the characteristics of the overall volcano-sedimentary sequence.

Acknowledgments A. C. Rebelo was supported by a grant SFRH/BD/77310/2011 from FCT (Fundação para Ciência e Tecnologia), Portugal. S. P. Ávila was supported by FCT Ciência 2008 contract. V. Zanon was funded by the Fundo Regional para a Ciência, through grant 03.1.7.2007.1 (PROEMPREGO Operational Program and Regional Government of the Azores). We thank Direcção Regional da Ciência, Tecnologia e Comunicações (Regional Government of the Azores), Clube Naval de Santa Maria, Câmara Municipal de Vila do Porto and all the participants of the several International Workshops "Palaeontology in Atlantic Islands" (2011–2015) for field assistance. This research also received substantial support from the SYNTHESYS Project (http://www.synthesys.info/), which is financed by European Community Research Infrastructure Action under the FP7 "Capacities" Program: A. C. Rebelo studied rhodoliths at the Natural History Museum London (GB-TAF-3394), B. Berning investigated type material of Azorean bryozoans (FR-TAF-1902, GB-TAF-3347), and S. P. Ávila studied the Miocene molluscs at the Museum für Naturkunde, Berlin (DE-TAF-1071). We thank Davide Bassi (Università di Ferrara) for the identification of the peyssonneliacean algae. Sincere thanks to C. Wimmer-Pfeil (Staatliches Museum für Naturkunde Stuttgart, Germany) and Anton Englert (Naturhistorisches Museum Wien) for thin-sections preparation and A. R. Mendes and J. Pacheco (CVARG, Universidade dos Açores) for laboratory assistance. We are also grateful to Editor-in-Chief Wolfgang Kiessling, reviewer Jochen Halfar and an anonymous reviewer for providing useful comments and suggestions that helped improve the final manuscript.

Appendix

See Table 4.

Table 4 Facies and stratigraphic assignment of logs

	Log A	Log B	Log C	Log D	Log F
Algae					
Hydrolithon sp.	2b, 3	2b, 3	2, 3	2	
Lithophyllum prototypum	2b, 3	2b, 3	2, 3	2	
Lithophyllum sp.	2b, 3	2b, 3	2, 3	2	
Phymatolithon calcareum	2b, 3	2b, 3	2, 3	2	
Phymatolithon sp.	2b, 3	2b, 3	2, 3	2	
Polystrata alba	2b, 3	2b, 3	2, 3	2	
Spongites sp.	2b, 3	2b, 3	2, 3	2	
Barnacles					
Zullobalanus santamariensis	2a, 3, 4		3	2	
Bryozoans					
Calloporina sp.	3	3	3		
Celleporiform spp. indet.	3	3	3		
Chaperiopsis sp.	3	3	3		
Escharina sp.	3	3	3		
Metrarabdotos sp.	3	3	3		
Microporella sp.	3	3	3		
Onychocella sp.	3	3	3		
Puellina spp.	3	3	3		
Reteporella sp.	3	3	3		
Rosseliana sp.	3	3	3		
Saevitella sp.	3	3	3		
Schizotheca sp.	3	3	3		
Scrupocellaria sp.	3	3	3		
Calcareous nannofossils		4, 5c, 6		4, 5c	
Calcidiscus leptoporus		4, 5c, 6		4, 5c	
Calcidiscus macintyrei		4, 5c, 6		4, 5c	
Cyclicargolithus floridanus		4, 5c, 6		4, 5c	
Coccolithus pelagicus		4, 5c, 6		4, 5c	
Coronosphaera sp.		4, 5c, 6		4, 5c	
Discoaster sp.		4, 5c, 6		4, 5c	
Helicosphaera carteri		4, 5c, 6		4, 5c	
Helicosphaera stalis		4, 5c, 6		4, 5c	
Pontosphaera sp.		4, 5c, 6		4, 5c	
Reticulofenestra antarticus		4, 5c, 6		4, 5c	
Reticulofenestra haqii-minutula		4, 5c, 6		4, 5c	
Reticulofenestra minuta		4, 5c, 6		4, 5c	
Reticulofenestra pseudoumbilicus		4, 5c, 6		4, 5c	
Reticulofenestra productus		4, 5c, 6		4, 5c	
Reticulofenestra rotaria		4, 5c, 6		4, 5c	
Sphenolithus sp.		4, 5c, 6		4, 5c	
Syracosphaera sp.		4, 5c, 6		4, 5c	
Umbilicosphaera jafari		4, 5c, 6		4, 5c	
Echinoids					
Clypeaster altus	2a, 2b		3	2, 5c	
Echinocardium sp.				5c	
Echinocyamus pusillus				5c	
Echinoneus cf. *cyclostomus*	3			5c	
Eucidaris tribuloides	2a, 2b, 3, 4	2b, 3	2, 3, 4	2, 5c	2a, 8
Spatangoida indet.	4			5c	

Table 4 continued

	Log A	Log B	Log C	Log D	Log F
Molluscs					
Anomia ephippium	3				
Arca noae	3				
Chlamys hartungi	3		3		
Chlamys varia	3	3			
Gigantopecten latissimus	3		3		
Lopha plicatuloides	3	2b	3		
Manupecten pesfelis	3	3	3		
Myoforceps aristatus	3				
Ostrea spp.	2a, 2b, 3	2b, 5b, 2b	2, 3	2, 5c	5a, 5b, 5c
Pecten dunkeri	3	2b	3	2	
Persististrombus coronatus				2, 5c	
Spondylus concentricus	3		3	2	
Spondylus gaederopus	2a			2	
Ostracods					
Aurila sp.				2, 4	
Callistocythere oertlii				2, 4	
Cyamocytheridea sp.				2, 4	
Dameriacella aff. *D. dameriacensis*				2, 4	
Heliocythere magnei				2, 4	
Leptocythere azorica				2, 4	
Loxoconcha rhomboidea				2, 4	
Loxoconcha stellifera				2, 4	
Neonesidea rochae				2, 4	
Pachycaudites aff. *P. armilla*				2, 4	
Paracypris sp.				2, 4	
?*Quadracythere* sp.				2, 4	
Xestoleberis cf. *paisi*				2, 4	
Trace fossils					
Bichordites isp.	5c			4, 6	
Dactyloidites ottoi				6	
Diopatrichnus isp.	4				
Entobia isp.	3				
Gastrochaenolites isp.	3				
Macaronichnus segregatis	4, 5c		4	2, 4, 5b, 6	
Macaronichnus isp.		6			
Ophiomorpha isp.	4, 5c	6	4	2, 4, 5b, 6	
Palaeophycus isp.	4, 5c			5b	
Piscichnus waitemata				4	
Piscichnus isp.	4	6	4	6	
?*Psilonichnus* isp.	4				
Thalassinoides isp.	4		4		

References

Aguirre J, Braga JC, Martín JM, Betzler C (2012) Palaeoenvironmental and stratigraphic significance of Pliocene rhodolith beds and coralline algal bioconstructions from the Carboneras Basin (SE Spain). Geodiversitas 34(1):115–136

Ávila SP, Madeira P, Zazo C, Kroh A, Kirby M, da Silva CM, Cachão M, Martins AMF (2009) Palaeoecology of the Pleistocene (MIS 5.5) outcrops of Santa Maria Island (Azores) in a complex oceanic tectonic setting. Palaeogeogr Palaeoclimatol Palaeoecol 274(1–2):18–31

Ávila SP, Ramalho R, Vullo R (2012) Systematics, palaeoecology and palaeobiogeography of the Neogene fossil sharks from the Azores (Northeast Atlantic). Ann Paléontol 98:167–189

Ávila SP, Melo C, Silva L, Ramalho R, Quartau R, Hipólito A, Cordeiro R, Rebelo AC, Madeira P, Rovere A, Hearty P, Henriques D, da Silva

CM, Martins AMF, Zazo C (2015a) A review of the MIS 5e high-stand deposits from Santa Maria Island(Azores, NE Atlantic): palaeobiodiversity, palaeoecology and palaeobiogeography. Quatern Sci Rev 114:126–148

Ávila SP, Ramalho R, Habermann J, Quartau R, Kroh A, Berning B, Johnson M, Kirby M, Zanon V, Titschack J, Goss A, Rebelo AC, Melo C, Madeira P, Cordeiro R, Meireles R, Bagaço L, Hipólito A, Uchman A, da Silva CM, Cachão M, Madeira J (2015b) Palaeoecology, taphonomy, and preservation of a lower Pliocene shell bed (coquina) from a volcanic oceanic island (Santa Maria Island, Azores, NE Atlantic Ocean). Palaeogeogr Palaeoclimatol Palaeoecol 430:57–73. doi:10.1016/j.palaeo.2015.04.015

Ávila SP, Melo C, Berning B, Cordeiro R, Landau BM, da Silva CM, Cachão M (2016) *Persististrombus coronatus* (Mollusca: Strombidae) in the lower Pliocene of Santa Maria Island (Azores, NE Atlantic): palaeoecology, palaeoclimatology and palaeobiogeographic implications. Palaeogeogr Palaeoclimatol Palaeoecol 441:912–923

Baarli BG, Cachão M, da Silva CM, Johnson ME, Mayoral EJ, Santos A (2014) A Middle Miocene carbonate embankment on an active volcanic slope: ilhéu de Baixo, Madeira Archipelago, Eastern Atlantic. Geol J 49:90–106

Basso D, Tomaselli V (1994) Palaeoecological potentiality of rhodoliths: a Mediterranean case history. In: Matteucci R et al. (ed) Studies on ecology and paleoecology of benthic communities. Boll Della Soc Paleontol Ital 2:17–27

Basso D, Nalin R, Campbell CS (2009) Shallow-water *Sporolithon* rhodoliths from North Island (New Zealand). Palaios 24:92–103

Bosence D (1976) Ecological studies on two unattached coralline algae from western Ireland. Palaeontology 19:71–88

Bosence D (1983) The occurrence and ecology of Recent rhodoliths—a review. In: Peryt TM (ed) Coated grains. Springer-Verlag, Berlin, pp 217–224

Bourrouilh-Le Jan FG, Hottinger LC (1988). Occurrence of rhodolites in the tropical Pacific—a consequence of mid-Miocene paleo-oceanographic change. In: Nelson CS (ed), Non-tropical shelf carbonates—modern and ancient. Sediment Geol 60:355–367

Braga JC, Aguirre J (2001) Coralline algal assemblages in upper Neogene reef and temperate carbonates in Southern Spain. Palaeogeogr Palaeoclimatol Palaeoecol 175:27–41

Braga JC, Vescogni A, Bosellini FR, Aguirre J (2009) Coralline algae (Corallinales, Rhodophyta) in western and central Mediterranean Messinian reefs. Palaeogeogr Palaeoclimatol Palaeoecol 275:113–128

Bromley RG, Asgaard U (1993) Two bioerosion ichnofacies produced by early and late burial associated with sea-level changes. Geol Rundsch 82:276–280

Bromley RG, Asgaard U, Jensen M (1997) Experimental study of sediment structures created by a spatangoid echinoid, *Echinocardium mediterraneum*. Proc Geol Assoc Lond 108:183–190

Buatois LA, Mángano MG (2011) Ichnology: organism-substrate interactions in space and time. Cambridge University Press, Cambridge, p 358

Cabioch J, Floch JY, Le Toquiton A, Boudouresque CF, Meinesz A, Verlaque M (1992) Guide des algues des mers d'Europe. Manche/Atlantique et Méditerranée. Ed. Delachaux et Niéstlé, 234 p

Checconi A, Bassi D, Carannante G, Monaco P (2010) Re-deposited rhodoliths in the Middle Miocene hemipelagic deposits of Vitulano (Southern Apennines, Italy): coralline assemblage characterization and related trace fossils. Sed Geol 225:50–66

de Gibert JM, Martinell J, Domènech R (1998) *Entobia* ichnofacies in fossil rocky shores, Lower Pliocene, northwestern Mediterranean. Palaios 13:476–487

Ferreira OV (1955) A fauna Miocénica da ilha de Santa Maria. Comun Serv Geol Port 36:9–44

Flügel E (2004) Microfacies of carbonate rocks. Analysis, interpretation and application. Springer, Berlin, p 976

França Z, Cruz JV, Nunes JC, Forjaz VH (2003) Geologia dos Açores: uma perspectiva actual. Açoreana 10:11–140

Gregory MR (1991) New trace fossils from the Miocene of Northland, New Zealand: *Rorschachichnus amoeba* and *Piscichnus waitemata*. Ichnos 1:159–205

Guiry MD, Guiry GM (2015) AlgaeBase. World-wide electronic publication, National University of Ireland, Galway. http://www.algaebase.org. Accessed 11 Nov 2015

Johnson ME, da Silva CM, Santos A, Baarli BG, Cachão M, Mayoral EJ, Rebelo AC, Ledesma-Vázques J (2011) Rhodolith transport and immobilization on a volcanically active rocky shore: Middle Miocene at Cabeço das Laranjas on Ilhéu de Cima (Madeira Archipelago, Portugal). Palaeogeogr Palaeoclimatol Palaeoecol 300:113–127

Johnson ME, Baarli BG, Cachão M, da Silva CM, Ledesma-Vázquez J, Mayoral EJ, Ramalho RS, Santos A (2012) Rhodoliths, uniformitarianism, and Darwin: Pleistocene and recent carbonate deposits in the Cape Verde and Canary archipelagos. Palaeogeogr Palaeoclimatol Palaeoecol 329–330:83–100

Johnson ME, Ramalho RS, Baarli BG, Cachão M, da Silva CM, Mayoral EJ, Santos A (2014) Miocene–Pliocene rocky on São Nicolau (Cape Verde Islands): contrasting windward and leeward biofacies on a volcanically active oceanic island. Palaeogeogr Palaeoclimatol Palaeoecol 395:131–143

Johnson ME, Ledesma-Vázquez J, Ramalho R, da Silva CM, Rebelo AC, Santos A, Baarli BG, Mayoral EJ, Cachão M (2016) Taphonomic range and sedimentary dynamics of modern and fossil rhodolith beds: Macaronesian realm (North Atlantic Ocean). In: Rhodolith/maerl beds: a global perspective. Springer, Berlin

Lee DE, Scholz J, Gordon DP (1997) Paleoecology of a late Eocene mobile rockground biota from North Otago, New Zealand. Palaios 12:568–581

Lund M, Davies PJ, Braga JC (2000) Coralline algal nodules off Fraser Island, eastern Australia. Facies 42:25–34

Madeira P, Kroh A, Martins AMF, Ávila SP (2007) The marine fossils from Santa Maria Island (Azores, Portugal): an historical overview. In: Ávila SP, Martins AMF (eds) Proceedings of the "1st Atlantic Islands Neogene", International Congress, Ponta Delgada, 12–14 June 2006. Açoreana Supl 5: 59–73

Madeira P, Kroh A, Cordeiro R, Meireles R, Ávila SP (2011) The fossil echinoids of Santa Maria Island, Azores (Northern Atlantic Ocean). Acta Geol Pol 61(3):243–264

Mayoral E, Ledesma-Vazquez J, Baarli BG, Santos A, Ramalho R, Cachão M, da Silva CM, Johnson ME (2013) Ichnology in oceanic islands; case study from the Cape Verde Archipelago. Palaeogeogr Palaeoclimatol Palaeoecol 381–382:47–66

Meireles RP, Faranda C, Gliozzi E, Pimentel A, Zanon V, Ávila SP (2012) Late Miocene marine ostracods from Santa Maria island, Azores (NE Atlantic): systematics, palaeoecology and palaeobiogeography. Rev Micropaléontol 55(4):133–148

Meireles RP, Quartau R, Ramalho RS, Rebelo AC, Madeira J, Zanon V, Ávila SP (2013) Depositional processes on oceanic island shelves—evidence from storm-generated Neogene deposits from the mid-North Atlantic. Sedimentology 60:1769–1785

Meireles RP, Keyser D, Ávila SP (2014) The Holocene to recent ostracods of the Azores archipelago (NE Atlantic): systematics and biogeography. Mar Micropaleontol 112:13–26

Miller KG, Kominz MA, Browning JV, Wright JD, Mountain GS, Katz ME, Sugarman PS, Cramer BS, Christie-Blick N, Pekar SF (2005) The Phanerozoic record of global sea-level change. Science 310(5752):1293–1298

Pemberton GS, Spila M, Pulham AJ, Saunders T., MacEachern JA, Robbins D, Sinclair IK (2001) Ichnology and sedimentology of shallow to marginal marine systems: Ben Nevis & Avalon

Reservoirs, Jeanne D'Arc Basin. Geological Association of Canada, Short course notes, 15, p 343

Pemberton SG, MacEachern JA, Dashtgard SE, Bann KL, Gingras MK, Zonneveld JP (2012) Shoreface. In: Knaust D, Bromley RG (eds) Trace fossils as indicators of sedimentary environments. Developments in Sedimentology, vol 64. Elsevier, Amsterdam, pp 563–603

Ramalho RS (2011) Building the Cape Verde Islands. Springer, Berlin, p 207

Ramalho RS, Quartau R, Trenhaile AS, Mitchell NC, Woodroffe CD, Ávila SP (2013) Coastal evolution on volcanic oceanic islands: a complex interplay between volcanism, erosion, sedimentation, sea-level change and biogenic production. Earth Sci Rev 127:140–170

Ramalho RS, Helffrich G, Madeira J, Cosca M, Quartau R, Thomas C, Hipólito A, Ávila SP (2014) The emergence and evolution of Santa Maria Island (Azores)—the conundrum of uplifting islands revisited. AGU Fall Meeting, San Francisco, 15–19 December: Abstract V11B-4697

Rasser M (1994) Facies and palaeoecology of rhodoliths and acervulinid macroids in the Eocene of the Krappfeld (Austria). Beitr Paläontol 19:191–217

Rebelo AC, Rasser MW, Riosmena-Rodríguez R, Neto AI, Ávila SP (2014) Rhodolith forming coralline algae in the Upper Miocene of Santa Maria Island (Azores, NE Atlantic): a critical evaluation. Phytotaxa 190(1):370–382

Rosas-Alquicira EF, Riosmena-Rodríguez R, Couto RP, Neto AI (2009) New additions to the Azorean algal flora, with ecological observations on rhodolith formations. Cah Biol Mar 50:143–151

Santos A, Mayoral E, Johnson ME, Baarli BG, da Silva CM, Cachão M, Ledesma-Vázquez J (2012) Basalt mounds and adjacent depressions attract contrasting biofacies on a volcanically active Middle Miocene coastline (Porto Santo, Madeira Archipelago, Portugal). Facies 58:573–585

Schlager W (2003) Benthic carbonate factories of the Phanerozoic. Int J Earth Sci 92:445–464

Seike K (2007) Palaeoenvironmental and palaeogeographical implications of modern *Macaronichnus segregatis* like traces in foreshore sediments on the Pacific coast of central Japan. Palaeogeogr Palaeoclimatol Palaeoecol 25:497–502

Serralheiro A (2003) A geologia da Ilha de Santa Maria, Açores. Açoreana 10:141–192

Serralheiro A, Madeira J (1990) Stratigraphy and geochronology of Santa Maria island (Azores). Livro Homenagem Carlos Romariz. Departamento de Geologia da Faculdade de Ciências da Universidade de Lisboa, Portugal, pp 357–376

Serralheiro A, Alves CAM, Forjaz VH, Rodrigues B (1987) Carta Vulcanológica dos Açores, Ilha de Santa Maria. Escala 1:15.000 (Folhas 1 e 2). (Ed. Serviço Regional de Protecção Civil dos Açores e Universidade dos Açores). Ponta Delgada, Portugal

Sibrant ALR, Hildendrand A, Marques FO, Costa ACG (2015) Volcano-tectonic evolution of the Santa Maria Island (Azores): implications for palaeostress evolution at the western Eurasia-Nubia plate boundary. J Volcanol Geoth Res. doi:10.1016/j.jvolgeores.2014.12.017

Sneed ED, Folk RL (1958) Pebbles in the lower Colorado River, Texas, a study in particle morphogenesis. J Geol 66:114–150

Steller DL, Foster M (1995) Environmental factors influencing distribution and morphology of rhodoliths in Bahia Concepción, B.C.S., Mexico. J Exp Mar Biol Ecol 194:201–212

Tucker ME (2003) Mixed clastic–carbonate cycles and sequences: quaternary of Egypt and carboniferous of England. Geol Croat 56:19–37

Uchman A, Johnson ME, Rebelo AC, Melo C, Cordeiro R, Ramalho R, Ávila SP (2015) Vertically-oriented trace fossil *Macaronichnus segregatis* from Neogene of Santa Maria Island (Azores; NE Atlantic. In: Mara, N. (Ed.), 13th International Ichnofabric Workshop, ichnofabric studies linking past, present, and future, Kochi, Japan, 14–21 May 2015, Abstract book, p 27

Uchman A, Johnson ME, Rebelo AC, Melo C, Cordeiro R, Ramalho R, Ávila SP (2016) Vertically-oriented trace fossil Macaronichnus segregatis from Neogene of Santa Maria Island (Azores; NE Atlantic) records a specific palaeohydrological regime on a small oceanic island. Geobios. doi:10.1016/j.geobios.2016.01.016

Wilmsen M, Niebuhr B (2013) The rosetted trace fossil *Dactyloidites ottoi* (Geinitz, 1849) from the Cenomanian (Upper Cretaceous) of Saxony and Bavaria (Germany): ichnotaxonomic remarks and palaeoenvironmental implications. Paläontol Zeitschr 88:123–138

Winkelmann K, Buckeridge JS, Costa AC, Dionisio MAM, Medeiros A, Cachao M, Avila SP (2010) *Zullobalanus santamariaensis* sp. nov. a new late Miocene barnacle species of the family Archeobalanidae (Cirripedia: Thoracica), from the Azores. Zootaxa 2680:33–44

Wisshak M, Form A, Jakobsen J, Freiwald A (2010) Temperate carbonate cycling and water mass properties from intertidal to bathyal depth (Azores). Biogeosciences 7:2379–2396

Wisshak M, Berning B, Jakobsen J, Freiwald A (2015) Temperate carbonate production: biodiversity of calcareous epiliths from intertidal to bathyal depths (Azores). Mar Biodivers 45:87–112

Woelkerling WJ, Irvine LM, Harvey A (1993) Growth-forms in non-geniculate coralline red algae (Corallinales, Rhodophyta). Aust Syst Bot 6:277–293

Zbyszewski G, da Veiga Ferreira O (1962) La faune Miocène 1078 de l'île de Santa Maria (Açores). Comun Serv Geol Port 46:247–289